Precambrian Research 364 (2021) 106364

Contents lists available at ScienceDirect

Precambrian Research

journal homepage: www.elsevier.com/locate/precamres

Early Svecofennian rift-related magmatism: Geochemistry, U-Pb-Hf zircon isotope data and tectonic setting of the Au-hosting Uunimäki gabbro, SW Finland

Jaakko Kara [a,*], Tuomas Leskelä [a,b], Markku Väisänen [a], Pietari Skyttä [a], Yann Lahaye [b], Markku Tiainen [b], Hanna Leväniemi [b]

[a] Department of Geography and Geology, University of Turku, Turku, Finland
[b] Geological Survey of Finland, Espoo, Finland

ARTICLE INFO

Keywords:
Geochronology
Geochemistry
Structural geology
Orogenic gold
Svecofennian orogeny
Tectonic switching

ABSTRACT

We characterise the geochemistry, zircon Lu-Hf composition, age and the structure of the Uunimäki gabbro (UGB) in south-western Finland to improve the understanding of i) the early Svecofennian (1.92–1.89 Ga) crustal evolution of the central Fennoscandian Shield, ii) the potential role of rift-related magmatism for the build-up of the Paleoproterozoic accretionary orogens and iii) evaluate, which geological features provide the primary control over the localization of an orogenic gold mineralisation. The zircon U-Pb geochronology defines an age of 1891 ± 5 Ma for the UGB, which is slightly older than most mafic intrusions in south-western Finland. The obtained chondritic initial zircon ε_{Hf} values with E-MORB type geochemical affinity suggest a sub continental lithospheric mantle source for the UGB. The overall geochemistry indicates that the UGB magma as well as other E-MORB type rocks in the Pirkanmaa and Häme belts were formed in a rift-related environment in a fore-arc region at 1.89 Ga, predated by arc-type magmatism at ~1.90 Ga and back-arc magmatism at ~1.92 Ga in the Tampere belt. Slab retreat due to roll-back is suggested to cause the extension and related magmatism in the fore-arc region. Moreover, the timing and compositional and isotopic changes of early-orogenic magmatism are broadly compatible with intervals of extension and contraction, i.e., a tectonic switching model, and may provide a perspective to rapid build-up of Paleoproterozoic crust. Structural characterisation provides a framework where gold mineralisations are preferentially located within the high-strain north-eastern domain of the UGB, within fracture networks adjoining the high-strain zones. Our results indicate that neither the geochemical composition nor age of the intermediate-mafic intrusive host rocks play a major role in controlling the formation of gold mineralisation. By contrast, the localization of orogenic gold is controlled by localised structures (shear zones, fractures), and the variation in lithological composition of the intrusive host may contribute to the style of the mineralisation.

1. Introduction

Rocks geochemically similar to mid-ocean ridge basalt (N-MORB) or enriched mid-ocean ridge basalt (E-MORB) are particularly useful in studying past geotectonic settings (e.g., Pearce and Cann, 1973; Wilson, 1989). The MORB signatures indicate major contributions from upper mantle and formation under extensional tectonic regimes within environments such as mid ocean ridge or back-arc spreading centres (e.g., Xia & Li, 2019). Moreover, geochemical and isotopic signatures among the MORB-rocks are useful not only to trace the petrogenetic features and source characteristics of the magmas but also to provide insight into the evolution of the mantle and the crust. Unfortunately, within Precambrian accretionary orogens the MORB type rocks are scarce by their volume (e.g., Cawood et al., 2009; Kemp et al., 2009), which is the case also for the Paleoproterozoic Svecofennian bedrock in central Fennoscandia, where mafic bodies have generally been attributed to 1.90–1.88 Ga early arc accretion (e.g., Kähkönen, 2005; Peltonen, 2005). However, a few identified occurrences of MORB-rocks in south-western Finland (e.g., Lahtinen, 1996; Sipilä & Kujala, 2014; Lahtinen et al., 2017) allow us to evaluate the potential role of rift-related

* Corresponding author.
E-mail address: jkmkar@utu.fi (J. Kara).

https://doi.org/10.1016/j.precamres.2021.106364
Received 18 January 2021; Received in revised form 12 August 2021; Accepted 12 August 2021
Available online 27 August 2021

magmatism for the build-up of the Svecofennian Orogen. However, only relative age relationships for the above mentioned MORB-type rocks have been determined (Lahtinen et al., 2017). Consequently, constraints particularly on their absolute ages, but also further geochemical characterization are required for their utilization in crustal modelling.

Another motivation for this study relates to understanding which geological features contribute to the formation of orogenic gold deposits in intrusive rocks: deformation zones and associated structures (such as tension veins) are known to provide primary control over the localization of mineralisations (Groves et al., 1998; Goldfarb and Groves, 2015). Furthermore, specific temporal periods of crustal evolution (Goldfarb et al., 2001) and geochemical composition of source rocks are associated with orogenic gold (Groves et al., 1998). By contrast, less is known about the role of variations within the age, lithology and geochemical composition of the (intrusive) host rocks for generation of orogenic gold deposits within the spatial and temporal scale of a tectonic province such as the Svecofennian crust of southern Finland.

We approach the above-mentioned issues through studying the gold-hosting Uunimäki gabbro (UGB; Kärkkäinen et al., 2016) showing E-MORB affinity, located in southern Finland (Fig. 1). We report here the modal compositions, whole rock geochemical compositions, zircon U-Pb ages and zircon Hf isotopes from the UGB and compare the data with the adjacent gold-hosting Jokisivu and Palokallio diorites/gabbros. Subsequently, we compare the composition of the UGB further with selected mafic igneous formations with E-MORB affinities in SW Finland to evaluate their geodynamic setting. Finally, we use field-mapping-based structural analysis of the UGB, together with the improved UGB characterization (geochemistry, isotopes, age), to address the question of the primary geological control over formation of gold mineralisations in intrusive rocks. A large number of gold mineralisations in southwestern Finland (Kärkkäinen et al., 2016; Tiainen et al., 2017) are available for comparison with the results of this study. These mineralisations occur frequently in the ~1.90–1.88 Ga intrusive rocks of intermediate-mafic compositions (Eilu, 2012; Eilu et al., 2016) and many are inferred to have a structural control (Saalmann et al., 2009; Saalmann et al., 2010; Mertanen & Karell, 2011; Mertanen & Karell, 2012).

The results of this investigation broaden the known age range of mafic intrusions of SW Finland and the versatility of geochemical signatures of Au-hosting intrusions. The geochemical results indicate that the UGB magmas were not formed in a subduction zone setting. Instead, we suggest a rift-related setting within a fore-arc region at 1.89 Ga for E-MORB type rocks in the Pirkanmaa and Häme belts. This was preceded by evolved arc-type magmatism at 1.90–1.89 Ga and E-MORB-type back-arc magmatism at ~1.92–1.90 Ga in the Tampere belt. The timing and compositional and isotopic variability/changes of early-orogenic magmatism are broadly compatible with intervals of extension and contraction, i.e., tectonic switching model (Collins, 2002a, b), and may provide a perspective to rapid build-up of Paleoproterozoic crust. Previously, the tectonic switching model have been adapted to south-central Sweden (Hermansson et al., 2008; Stephens and Andersson, 2015) and to southern Finland at 1.86–1.78 Ga (Saalmann et al., 2009). This study extends the model of Saalmann et al. (2009) to 1.92–1.86 Ga and provides new geochemical and isotopical perspectives and new age constraints to the model. Moreover, the results indicate that the role of structural evolution in controlling the localization of orogenic gold overrides that of the host rock age or geochemical composition.

2. Geological background

2.1. Svecofennian orogen

The Paleoproterozoic Svecofennian orogen in the central Fennoscandian Shield represents the northern part of the East European Craton (Gorbatschev & Bogdanova, 1993) and is separated from the Archean Karelian Province by a NW-SE striking suture zone (Fig. 1a; Koistinen, 1981; Lahtinen et al., 2015). The Svecofennian orogen is

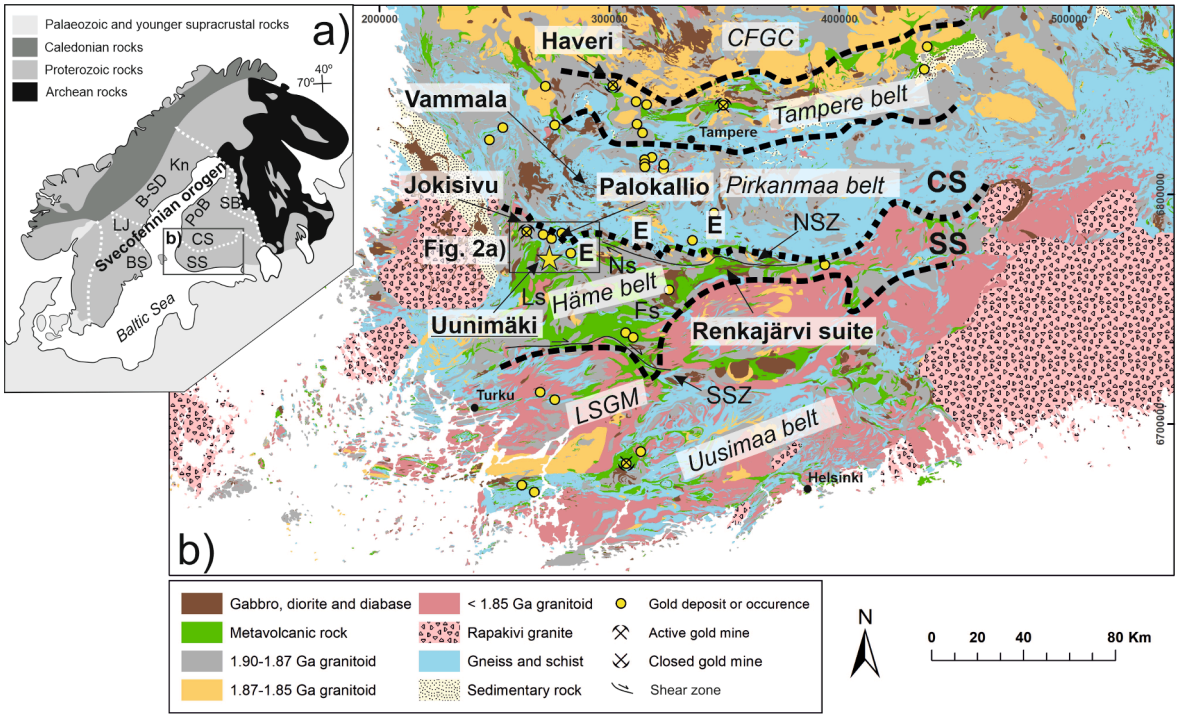

Fig. 1. a) Geological overview of the Fennoscandian Shield, modified after Koistinen et al. (2001). CS = Central Svecofennia, SS = Southern Svecofennia, SB = Savo belt, PoB = Pohjanmaa belt, Kn = Knaften-Barsele arc, B-SD = Bothnia–Skellefte lithotectonic unit, LJ = Ljusdal lithotectonic unit, BS = Bergslagen lithotectonic unit. b) Lithological map of southern Finland, modified after Bedrock of Finland – DigiKP. The study area is indicated by a black rectangle. CFGC = Central Finland Granitoid Complex, LSGM = Late Svecofennian granite-migmatite zone, Fs = Forssa suite, Ls = Loimaa suite, Ns = Nuutajärvi suite, E = Pirkanmaa belt E-MORB, NSZ = Nuutajärvi shear zone, SSZ = Somero shear zone. North is up in both maps; coordinates are in EUREF-FIN-TM35FIN in map b).

characterised by igneous rocks with ages at 1.96–1.80 Ga (e.g., Wasström, 1993; Nironen, 1997; Lahtinen et al., 2009a; Stephens and Andersson, 2015; Nironen, 2017) and is suggested to consist of several terranes and lithotectonic units in Finland and Sweden. In Finland at least three stacked terranes are recognised, which were accreted to the Archean craton during the Svecofennian orogeny: the Savo belt, Central Svecofennia and Southern Svecofennia (e.g., Korsman et al., 1997). The northern part of Central Svecofennia is characterised by the granitoid-dominated Central Finland granitoid complex (Nironen, 2005), whereas the southern part can be divided into the medium-metamorphic-grade volcano/sedimentary Tampere belt and high-grade sedimentary Pirkanmaa belt (Kähkönen, 2005). Southern Svecofennia is divided to two E-W trending volcanic belts, the Häme belt in the north and Uusimaa belt in the south, which are separated by the late Svecofennian granite-migmatite zone (Fig. 1b; Ehlers et al., 1993; Korsman et al., 1997; Kähkönen, 2005 and references therein; Lahtinen et al., 2009a).

There is a wide agreement of an accretionary nature of the Svecofennian orogen (e.g., Gaál & Gorbatschev, 1987; Lahtinen et al., 2005, 2009a; Hermansson et al., 2008; Saalmann et al., 2009; Nironen, 2017) and two main tectonic models have been presented for the Svecofennian orogen. The first model involves combined accretionary and collisional processes with collision of arc complexes and microcontinents against the Archean continent (Nironen, 1997; Lahtinen et al., 2005; Korja et al., 2006). The model includes several orogenies, involving microcontinent accretion, continental extension, continental collision and orogenic collapse prior to crustal stabilization (Lahtinen et al., 2005, 2009a; Nironen, 2017). A refined model includes buckling of an originally linear orogen into a curved orocline (Lahtinen et al., 2014, 2017). The second model emphasises accretionary processes in single active continental margin (Rutland, et al., 2004; Williams et al., 2008) and accretion of several island arcs (Bogdanova et al., 2015) or subduction beneath an active continental margin in combination with hinge retreat and advance resulting in tectonic switching between contractional and extensional tectonics (Hermansson et al., 2008; Saalmann et al., 2009; Stephens & Andersson, 2015). Chopin et al., (2020) combined the orocline buckling model within a single continental margin to account for the tectonic evolution of the central part of the Svecofennian orogen. It must be noted that majority of the models do not spatially nor temporally cover the whole Svecofennian orogen and evidence for both main tectonic models are found regionally and locally. Therefore, the question of the tectonic evolution remains open.

2.2. The Häme, Pirkanmaa and Tampere belts

The bedrock of the Häme belt in SW Finland was mainly formed at 1.88–1.87 Ga (Lahtinen et al., 2005). It consists of volcanic and sedimentary rocks (Lahtinen, 1996; Kähkönen, 2005) that have metamorphosed in amphibolite facies (Hölttä & Heilimo, 2017). The supracrustal rocks are intruded by 1.88–1.87 Ga gabbros, diorites, granodiorites and tonalites (Suominen, 1988; Nironen, 1999; Kähkönen, 2005; Saalmann et al., 2010; Tiainen et al., 2013; Mäkitie et al., 2016) and late- to post-tectonic (1.85–1.79 Ga) granites, migmatites and pegmatites (Nironen et al., 2016, 2017a). The supracrustal and plutonic rocks cover approximately equal area at present erosion surface (Bedrock map of Finland – DigiKP; Nironen et al., 2017a). The volcanic rocks of the Häme belt were divided into four main suites by Sipilä & Kujala (2014): the Forssa, Loimaa, Nuutajärvi and Renkajärvi suites. The calc-alkaline Forssa volcanic suite ranges from basaltic to rhyolitic, andesites being the most common. The calc-alkaline Loimaa suite consists mostly of amphibolites and hornblende-gneisses and the protolith compositions are less constrained due to stronger metamorphic overprint compared to the Forssa suite. The Nuutajärvi suite differs lithologically from other units in Häme belt, consisting mostly of sedimentary and calc-alkaline felsic volcanic rocks. Rocks of the Renkajärvi suite have an E-MORB-affinity and consist of mafic and intermediate volcanic rocks (Lahtinen, 1996; Sipilä & Kujala, 2014). The volcanic rocks are often associated with plutonic rocks, which might represent magma chambers to the former (Suominen, 1988; Peltonen, 2005; Sipilä & Kujala, 2014).

The Pirkanmaa belt is dominated by migmatised psammitic supracrustal rocks of turbiditic origin deposited at 1.92–1.89 Ga (Huhma et al., 1991; Kähkönen, 2005; Lahtinen et al., 2009b). The supracrustal rocks are intruded by small ultramafic to mafic plutonic bodies with arc or transitional MORB affinities, which were interpreted as synorogenic conduits of tholeiitic arc-type magmas (Peltonen, 1995, 2005). It also includes minor ultramafic (picritic) to mafic volcanic rocks with MORB to WPL affinities (Peltonen, 1995; Lahtinen, 1996; Kähkönen, 2005) and various synorogenic granitoids (Nironen & Bateman, 1989) and minor black shales (Lahtinen et al., 2017). The granitoids comprise 1.89–1.87 Ga tonalites, quartz diorites and granodiorites (Nironen, 1989; Nironen & Bateman, 1989; Kilpeläinen, 1998; Nironen, 2005). Local metamorphism is characterised by high temperature and low pressure and is dated at ~1.88 Ga (Mouri et al., 1999; Rutland et al., 2004; Lahtinen et al., 2009b). The medium-grade Tampere belt is situated north of the Pirkanmaa belt and is characterised by volcanic rocks formed in volcanic arc environment 1.91–1.89 Ga ago (Kähkönen, 2005). It has been interpreted that the Pirkanmaa belt is a mid-crustal expression of a fore-arc and an accretionary prism/subduction complex to the Tampere belt volcanic arc complex (Lahtinen, 1996; Kähkönen, 2005; Lahtinen et al., 2009b).

Mafic rocks with MORB signature are rare in southern Finland. The Renkajärvi volcanic suite, located in the NE part of the Häme Belt, is mainly composed of mafic volcanic rocks stratigraphically on top of the sedimentary rocks (Sipilä & Kujala, 2014). The picritic lavas in Vammala within the Pirkanmaa belt occur as intercalations in sedimentary rocks and are spatially associated by small tholeiitic igneous bodies (Peltonen 1995). Peltonen (1995, 2005) considered that the mafic bodies are related to 1.90–1.87 Ga early arc accretion and are younger than the picritic lavas so the two types are not related. The Pirkanmaa belt comprises also other volcanic rocks with E-MORB affinities (Sipilä & Kujala, 2014; Lahtinen et al., 2017), which are geochemically rather diverse and spatially dispersed. These volcanics show pillow structures in places. The Haveri Au-Cu deposit is located in northern edge of the arc-type Tampere belt and consists of mafic metalavas with E-MORB affinities (Eilu, 2012). Kähkönen (1999; 2005) considered that Haveri is the lowermost unit in the Tampere belt formed in submarine conditions in an extension-related setting based on the tholeiitic pillow lavas and depositional structures in sedimentary rocks. A back-arc setting was suggested by Strauss (2004) but poorly defined age, in addition to the fact that rocks predating the Haveri have not been found, make these interpretations unclear. There are E-MORB type basalts and picrites also in the Orijärvi (Väisänen & Mänttäri 2002, Nironen 2017b) and transitional-MORB type rocks in Turku and Pargas areas (Väisänen & Westerlund, 2007), but these are regarded to belong to another volcanic arc system, the Uusimaa belt. So far, no absolute age determination on the (E-)MORB-type rocks/formations exists and the ages are based only on field relations.

Major E-W trending shear zones (SZs), the Nuutajärvi SZ and the Somero SZ may act as dividing boundaries between the Pirkanmaa, Häme and Uusimaa belts, respectively (Fig. 1; Nironen et al., 2017a), but terrane boundaries are difficult to define (Kähkönen, 2005; Sipilä et al., 2011). These shear zones were developed after the peak metamorphism (Nironen, 1999; Lahtinen et al., 2005; Saalmann et al., 2010). The shearing was localized into E-W, NE-SW and NW-SE trending shear zones throughout the Häme belt, and N-S trending shear zones further in the west (Nironen, 1999; Väisänen & Skyttä, 2007; Pitkälä, 2019).

Comparison of the Pirkanmaa and Häme belts and the intervening Loimaa area shows (Fig. 1) that the similar relationships between the intrusive events and main deformation stages prevailed: the maximum age of the earliest deformation is constrained at around 1.89 Ga in the Pirkanmaa belt using correlation of depositional ages and penetrative

deformation fabrics (Nironen, 1989; Kilpeläinen, 1998). The age of the main deformation (D2 by Kilpeläinen, 1998) is constrained by the voluminous *syn*-tectonic intrusives at 1885–1880 Ma (Nironen, 1989; Kilpeläinen, 1998, Saalmann et al., 2010). More localized structural overprint was associated with intrusion of (porphyritic) granitoids at 1.87 Ga (Nironen, 1999; Kilpeläinen, 1998). Contrasting to the Pirkanmaa belt, which lacks distinct post-1.87 Ga deformation, localized deformation characterised by folds and particularly shear zones and faults has been documented within the Loimaa and Häme areas (Nironen, 1999; Saalmann et al., 2010).

The orogenic gold mineralisations in southern Finland are spatially associated with quartz veins (e.g., Eilu, 2012) and local alteration such as sulfidisation (Kärkkäinen & Tiainen, 2016). The quartz veins trend to sub-vertical fault or shear systems attributed to the WNW-ESE crustal shortening during the late stages (1.83–1.78 Ga) of orogenic evolution at or after the transition to the brittle tectonic regime (Saalmann, 2007, Saalmann et al., 2009, 2010). Regionally, the gold occurrences are distributed along a NW-SE trend, whereas in the local scale, gold is controlled by WNW–ESE- and WSW–ENE, SW-NE to WSW-ENE and NW-SE, second- or third-order shear zones and faults, which represent branches from regional-scale NW-SE-trending shears (Saalmann et al., 2009).

2.3. The Uunimäki area

The Uunimäki prospect is located in the north-western part of the Häme belt, where the bedrock consists of mica gneisses, mafic volcanic rocks, granitoids and mafic plutonic rocks (Fig. 2; Kärkkäinen et al., 2016). The gold-hosting Uunimäki gabbro (Fig. 2a, b; UGB) is exposed as a 1000 × 700 m oval-shaped intrusion located close to the termination of the ENE-WSW trending transpressional Kankaanranta shear zone (Fig. 3a; Leskelä, 2019). In the east, the Kankaaranta shear zone is possibly linked to the E-W trending Nuutajärvi shear zone (Fig. 1). The UGB shows local alteration characterized by albitisation, sulfidisation, chloritisation, sericitisation and the formation of epidote, quartz veins and carbonate veins (Fig. 4a; Kärkkäinen & Tiainen, 2016).

Gold was discovered by the GTK in 2008 in connection with evaluation of gold potential in mafic intrusions intersected by fault and shear zones (Kärkkäinen et al., 2016). The discovery was followed by geophysical (Huotari-Halkosaari et al., 2016) and basal till geochemistry surveys, a drilling campaign (with 36 drill holes and a total of 3425 m drilled; Kärkkäinen et al., 2016) and ore mineralogy studies (Kärkkäinen et al., 2015) conducted by GTK. Gold-rich (>1 ppm) sections were discovered in 27 of the holes (Kärkkäinen et al., 2016). The highest concentrations of gold/m were found in holes R8 (15.0 ppm), R23 (35.2 ppm) and R25 (38.4 ppm; Fig. 3b). Most of the drilling was done in NW Uunimäki and the holes were drilled towards the SW with an azimuth of 225 and a plunge of 45 (Fig. 3b).

Several vein generations occur including multiple quartz and silicate veins, sulfide-silicate and sulfide veins but usually their relations are somewhat unclear (Fig. 4b and c; Kärkkäinen et al., 2016). The gold is associated with silicates and sulfides; thin pyrrhotite vein networks, sporadic pyrrhotite-hornblende veins and pure quartz veins with native gold have the highest gold concentrations (Fig. 4b-e). Gold occurs as complex grains with Bi, Bi-sulfide, Bi-Te minerals and arsenopyrite as well as native gold grains (Fig. 4f-h; Kärkkäinen et al., 2015). Chalcopyrite is present as well, but it is considered to be of primary magmatic origin (Kärkkäinen et al., 2015). The gold mineralisation within the UGB is interpreted to be related to a complex network of fracture and shear zones, formed in a semi-ductile environment, where NW-SE-trending ones have been the gold mineralisation controlling structures (Fig. 3b; Kärkkäinen et al., 2016). Gold within this structural network shows distinct zoning with highest concentrations into the seemingly unaltered gabbro with only thin pyrrhotite veins and narrow hornblende rich bands (Fig. 4b and c), whereas the spatially adjoining sheared and fractured parts of the gabbro, representing most intense mechanical and

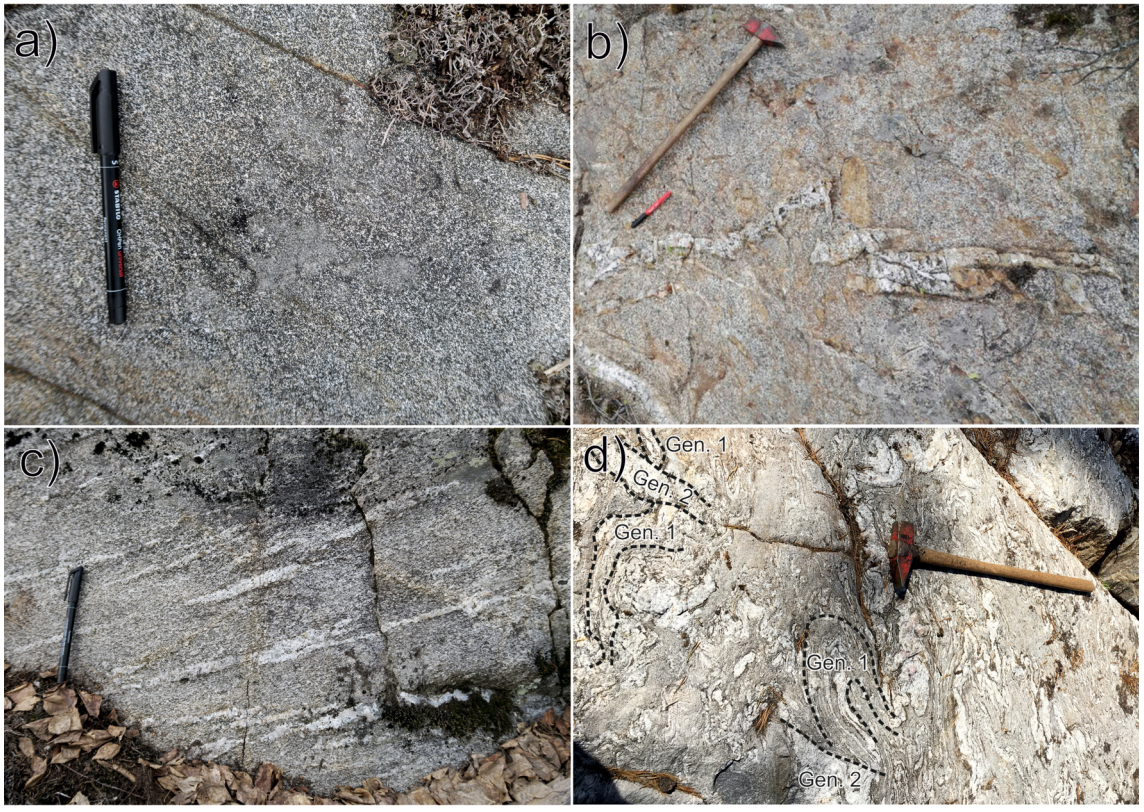

Fig. 2. Field photos of Uunimäki rock types. a) Undeformed Uunimäki gabbro (TALE-2017–17.1), b) deformed gabbro crosscut by rusty quartz veins, c) foliation parallel quartz veins in Uunimäki quartz diorite and d) local paragneiss showing two leucosomes generations.

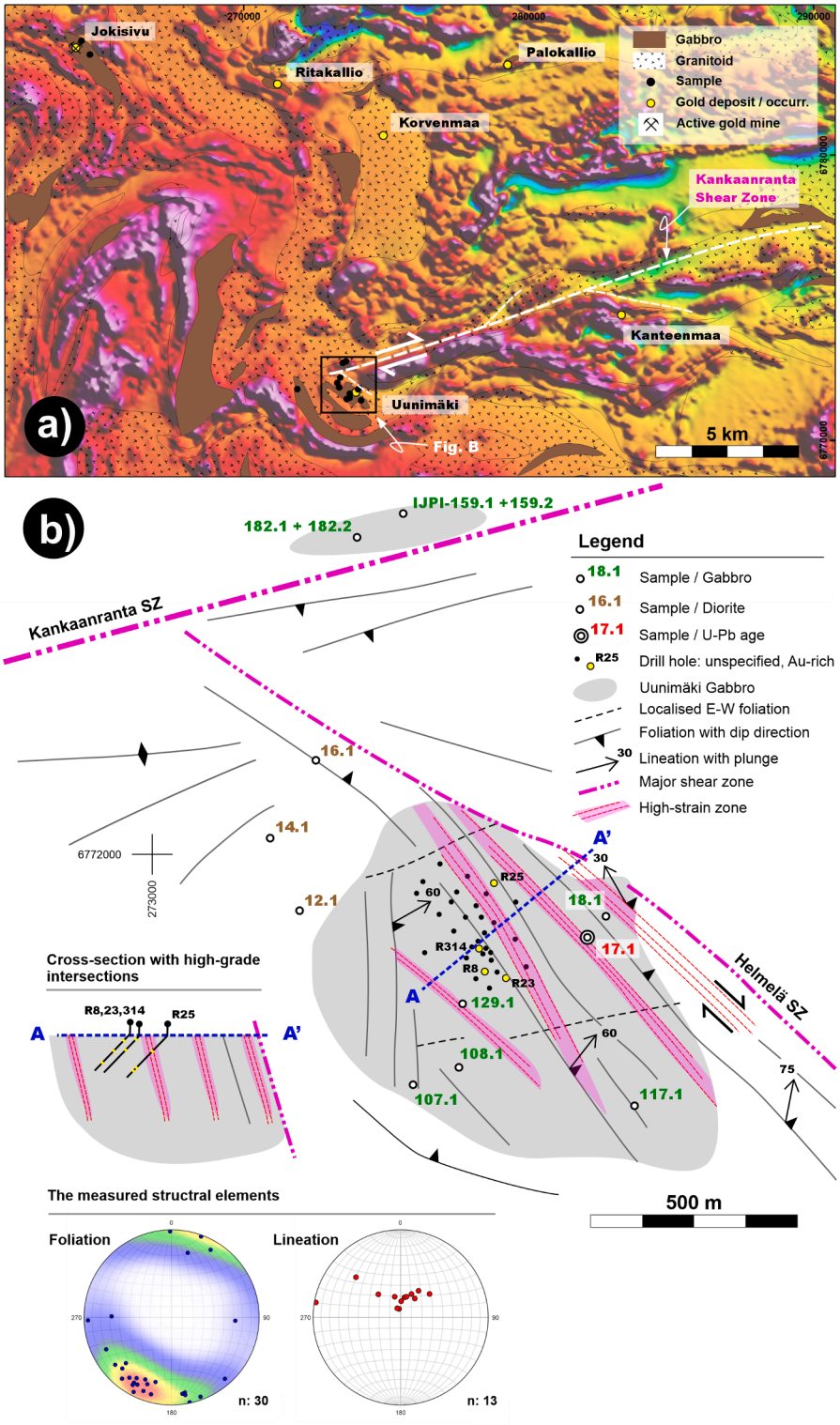

Fig. 3. a) An overview of the gold mineralisations, structural trends (as shown by the aeromagnetic data) and the gabbroic bodies within the area of investigation. Aeromagnetic data from GTK. b) Structural interpretation of the Uunimäki gabbro, including a schematic cross-section with projected high-grade gold drill hole intersections and lower hemisphere stereographic projections illustrating orientation distribution of the dominant foliation (grain shape fabrics) and mineral lineation. The existing drilling sites (collars), as well as samples taken in this study area indicated. North is up in both maps; coordinates are in EUREF-FIN-TM35FIN.

chemical alteration, and NW trending granite pegmatite dykes display sulfidic alteration but no gold mineralisation (Fig. 4a).

3. Materials and methods

The materials for this study consist of field observation data which, supported by aeromagnetic maps and petrographic observations, we used to generate revised lithological and structural maps of the UGB and its immediate surroundings. We collected a total of fifteen samples, eight from the UGB and seven from the adjacent Uunimäki quartz diorite and analysed the samples for whole rock geochemistry (Figs. 2 and 3b). Most samples are homogeneous, reflecting the primary magmatic character of the rocks, whereas a few are expected to be altered as they were collected near contacts with other rock types or close to shear zones. Single-grain zircon U-Pb age determination and zircon Lu-Hf analysis were conducted on sample (TALE-2017–17.1) representing fresh and

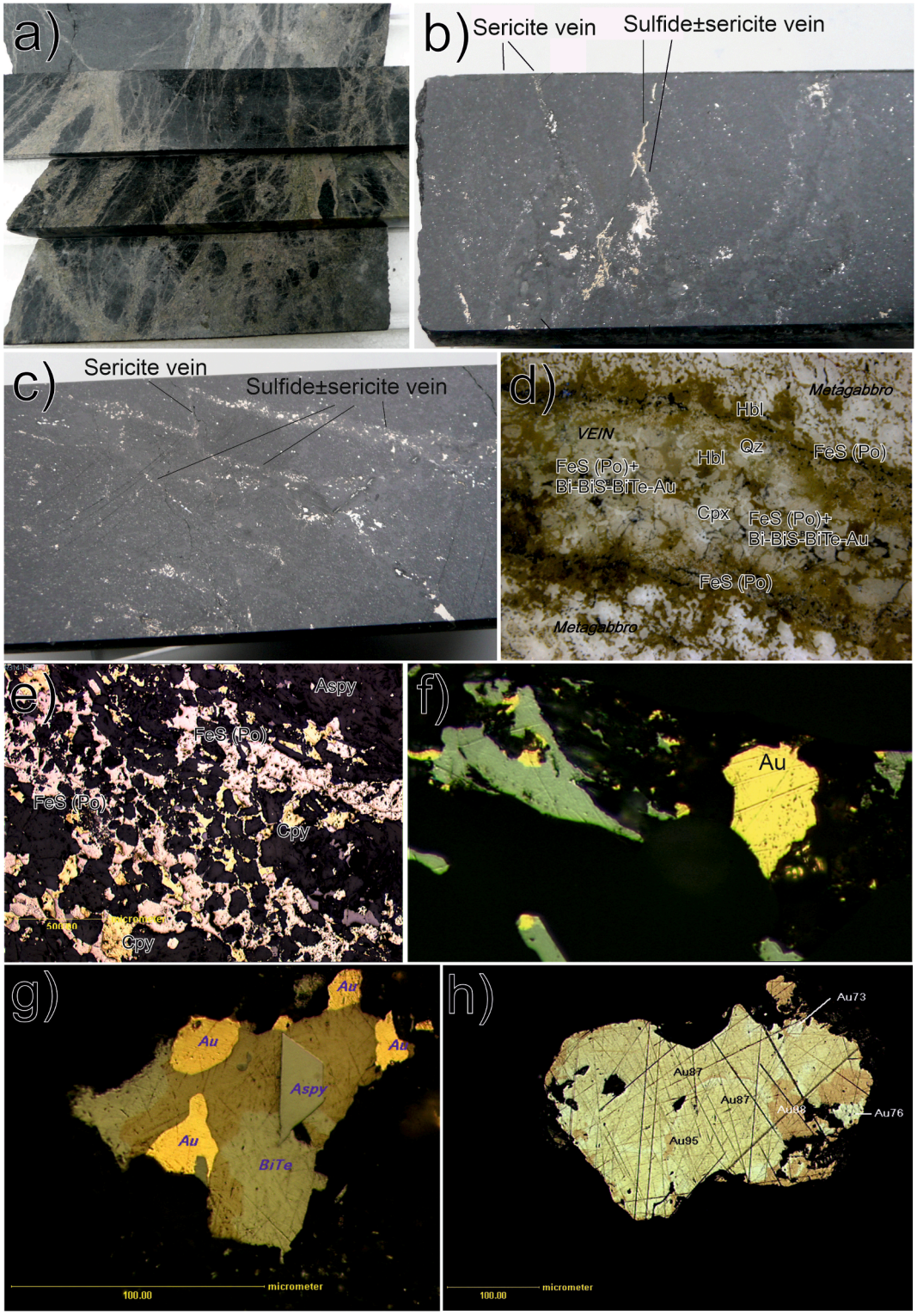

Fig. 4. Macro and microphotographs showing alteration and mineralisation styles of the UMG. a) Non-mineralised section of shear brecciated UMG showing a network of light sericite-epidote-carbonate veins and altered host rock (drillhole R314); b) Au-mineralised gabbro with sulfide veins (pyrrhotite ± arsenopyrite, chalcopyrite), which are cross-cut by younger sericite veins. Pyrrhotite and chalcopyrite are partly remobilised into sericite veins (drillhole R25); c) several generations of sulfide veins (pyrrhotite ± arsenopyrite), which are cross-cut by thin younger sericite vein (drillhole R25); d) microphotograph of 10 mm thick Au-mineralised silicate-sulfide vein (pyrrhotite-hornblende-clinopyroxene). The vein is rimmed by hornblende and pyrrhotite, shows clinopyroxene rich core and contains native gold and bismuth, several Bi and Te minerals and arsenopyrite (drillhole R314); e) microphotograph of slightly Au-mineralised pyrrhotite-chalcopyrite vein (drillhole R314); f) native gold grains in a quart vein (drillhole R314); g) a complex grain of Au, Bi-Te minerals and arsenopyrite (drillhole R314); h) a complex Au grain showing variable Au content between 73 and 95 %). Abbreviations: Po = pyrrhotite, Cpy = Chalcopyrite, Aspy = arsenopyrite, Cpx = clinopyroxene, Hbl = hornblende, Qz = quartz. The photos are modified after Kärkkäinen et al., (2015) and Kärkkäinen et al., (2016).

homogeneous variety of the UGB. The analytical methods are described in Electronic Appendix A.

For comparative studies we collected and analysed five samples from the Jokisivu diorite, hosting an active Au-mine and twelve previously published samples from the Palokallio gold prospect (Voipio, 2008). For wider regional comparisons aiming at clarifying the geotectonic environment of the studied rocks, we additionally used previously published E-MORB-type mafic rocks from SW Finland (Peltonen 1995; Strauss, 2004; Sipilä and Kujala, 2014; Lahtinen et al., 2017).

4. Results

4.1. Petrography of the Uunimäki area

4.1.1. Gabbro

The Uunimäki gabbro (UGB) is dark-grey, medium-grained and equigranular rock (Fig. 2a and 5a), though finer-grained varieties were observed on some outcrops. The gabbro is crosscut by quartz veins (Fig. 2b), hornblende-rich mafic veins, quartz-feldspar veins, carbonate veins (Fig. 4a-d) and, rarely, pegmatite dykes. Magmatic layering is visible on some outcrops, and the gabbro contains cumulus-textured peridotitic enclaves, visible on outcrops and drill cores (Kärkkäinen et al., 2016).

The UGB is a hornblende gabbro comprising plagioclase, hornblende and biotite as primary minerals (Fig. 5), with pyroxene observed in some drill cores (Fig. 4d; Kärkkäinen et al. 2016). Accessory minerals include ilmenite and rare pyrrhotite. Zircons are not common but are present as inclusions in a few biotite grains (Fig. 5). Plagioclase compositions determined from five thin sections gave anorthite content of An_{55}-An_{60} (labradorite; optical method). Minor alteration of the intact gabbro can be seen by sericitisation of plagioclase and chloritisation on the edges of biotite and amphibole (Fig. 5), whereas the sheared parts show strong alteration (Fig. 4a; Kärkkäinen & Tiainen, 2016).

4.1.2. Quartz diorite

The Uunimäki quartz diorite has > 5% modal quartz and is therefore classified as quartz diorite. This rock is medium-grained, equigranular, and the colour ranges from grey and brownish-grey. The primary minerals are plagioclase, biotite and quartz. K-feldspar is also locally present. Hornblende are present as accessory minerals, with some opaque minerals. The quartz diorites are typically well-foliated and commonly have small mafic microgranitoid enclaves (MGEs) elongated parallel to the foliation. Quartz veins are locally present parallel to the main foliation, with rare aplite and pegmatite veins crosscutting the dominant structural features. The quartz diorite outcrops near the UGB frequently display high-strain fabrics and are intruded by quartz veins (Fig. 2c).

The composition of the plagioclase in the quartz diorites varies between An_{35} and An_{50} (andesine; optical method). Biotites are elongated and have apatite and zircon inclusions. K-feldspar grains, when present, are often clearly coarser than the rest of the grains, making the rock locally porphyritic.

4.1.3. Paragneisses

The primary minerals of the paragneisses are biotite, quartz and plagioclase and the grain size is ~2–5 mm. The fraction of leucosome varies from none to > 50% depending mostly on the composition. Two leucosome generations was observed: one that was folded with the paragneiss, and a later one intruded into the axial plane of the folding (Fig. 2d).

A sample from a ten of metres wide migmatitic paragneiss inclusion within the quartz diorite intrusion contains a metamorphic mineral paragenesis biotite-cordierite-garnet. Sillimanite needles occur as inclusions in cordierite. These indicate the upper-amphibolite to lower-granulite facies metamorphism (e.g., Young et al., 1989).

4.2. The structural framework of the Uunimäki area

The UGB is structurally characterized by strain localization into spaced NW-SE trending high-strain zones, which transect low-strain rocks displaying weak to moderate, typically NW-SE trending grain shape fabrics (Fig. 3b). The high-strain zones occur predominantly within the north-eastern part of the UGB, and they have a parallel orientation with the Helmelä shear zone occurring along the north-eastern contact of the UGB. The high-strain zones are associated with development of linear topographic depressions, increased foliation intensity and decreased grain size of the gabbro, as well as the change of the rock colour from dark grey to pale brown or greenish as response to hydrothermal alteration (Fig. 3a, b). Foliations within the low- and high-strain zones are steep to sub-vertical and dip dominantly towards NE. Mineral lineations within the high-strain zones plunge gently-moderately towards NW and are indicative of strike- to oblique-slip movement. By contrast, lineations within the low-strain rocks plunge moderately-steeply down-dip, towards NE-NNE (Fig. 2b). More localized deformation fabrics are present as sub-vertically dipping planar fabrics which trend ENE-WSW, parallel with the Kankaanranta shear zone. Further, a discrete N-S trending topographic depression associated with steeply east-dipping foliation occurs within the western part of the UGB. Foliation trends within the quartz diorites surrounding the UGB are sub-parallel with the dominant NW-SE trends of the UGB in the south-east, whereas towards the Kankaanranta SZ in the north they display dominantly ENE-WSW orientations. Contact relations between the UGB, the hosting supracrustal rocks or the Uunimäki diorite are not exposed.

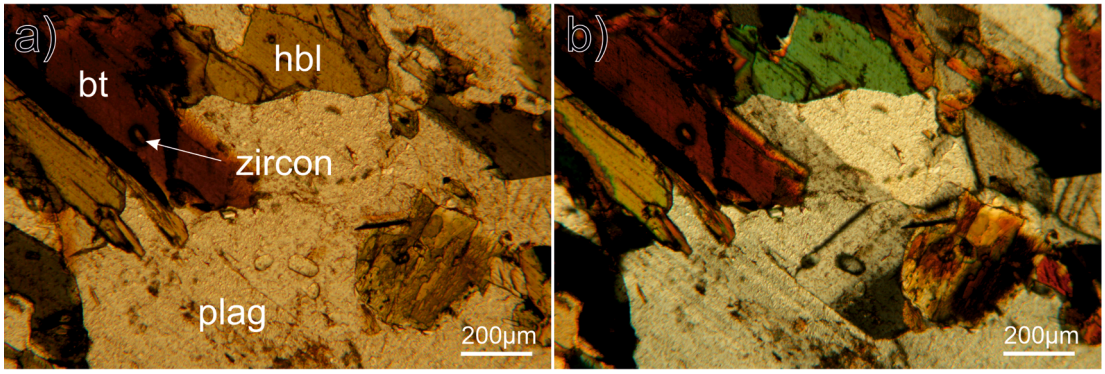

Fig. 5. Photomicrographs (plane-polarized on left and cross-polarized on right) of the Uunimäki gabbro showing zircon enclosures with pleochroic halos in biotite in the age sample TALE-2017–17.1. Abbreviations: hbl = hornblende; plag = plagioclase; bt = biotite.

4.3. Geochemistry

4.3.1. Major elements

SiO_2 content of the UGB samples vary between 48 and 52 wt% and they are classified as gabbros in the total alkali vs. silica -diagram (TAS; Fig. 6a). Two of the gabbro samples (TALE-2017–182.2 and IJPI-2017–159.2), collected near the ENE-WSW Kankaanranta shear zone, show slightly higher SiO_2 and alkali contents indicating alteration. In the immobile trace element classification diagram (Fig. 6b), the samples form tight cluster and are classified as basalts. The UGB is metaluminious (Fig. 6c) and plots in the tholeiitic field in the TAS diagram (Fig. 6a). The UGB shows MgO content of 4–6 wt% and Fe_2O_3 is abundant (>11 wt%; Harker diagrams for selected major elements are shown in Electronic Appendix C). CaO and Al_2O_3 contents are rather high and uniform (>8.4 wt% and > 16.8 wt%, respectively). K_2O, Na_2O and P_2O_5 contents are low (<1.3 wt%, <3.2 wt% and < 0.29 wt%, respectively) but TiO_2 is rather high (>1.3 wt%).

SiO_2 contents of the quartz diorites range between 56 and 65 wt% and four of the samples are classified as diorites, two as granodiorites and one as monzonite in the TAS-diagram (Fig. 6a). However, the dioritic samples contain quartz, the two granodioritic samples are regarded to have gained extra silica in an alteration process and the monzonite sample and one dioritic samples are also considered altered. In the immobile trace element classification diagram, the samples straddle between trachyandesite and andesite fields with one alkali basalt outlier (Fig. 6b). The quartz diorites are both metaluminious and peraluminous (Fig. 6c). MgO and Fe_2O_3 contents are rather low (<4.5 wt% and < 8.6 wt%, respectively). Four samples show Al_2O_3 contents of 15–18 wt%, but one sample (TALE-2017–12.1) shows as high as 19.7 wt%. CaO content ranges between 4.6 and 6.2 wt%. Na_2O contents for four samples vary between 3 and 4 wt%, except that one outlier (IJPI-2017–159.1) is only 1.3 wt%. K_2O contents of the samples range between 1.6 and 2.5 wt-%. TiO_2 and P_2O_5 contents are rather low (<0.3 wt % and < 1.2 wt%, respectively).

The samples from Jokisivu plot neatly into the gabbroic diorite field, while the Palokallio samples are more scattered and plot into the gabbroic diorite, diorite, monzodiorite and monzonite fields (Fig. 6). In term of major elements, the Jokisivu and Palokallio samples fill the gap between the UGB and the Uunimäki quartz diorite samples forming a linear trend between the two groups.

4.3.2. Trace elements

The UGB shows homogeneous trace elements content (Harker diagrams for selected trace elements are shown in Electronic Appendix C) except the two altered samples (TALE-2017–182.2 and IJPI-2017–159.2). The large ion lithophile element (LILE) contents are low, especially Th, but Sr is high in all samples. Cr and Ni contents are rather low. The UGB is slightly enriched in high field strength elements (HFSE) with Nb content of 8–12 ppm and Y content of 19–26 ppm. There is some variation in the Zr content, which varies between 59 and 125 ppm. F content ranges between 257 and 432 ppm, except for the altered sample IJPI-2017–159.2, which has F content of 627 ppm. The UGB samples

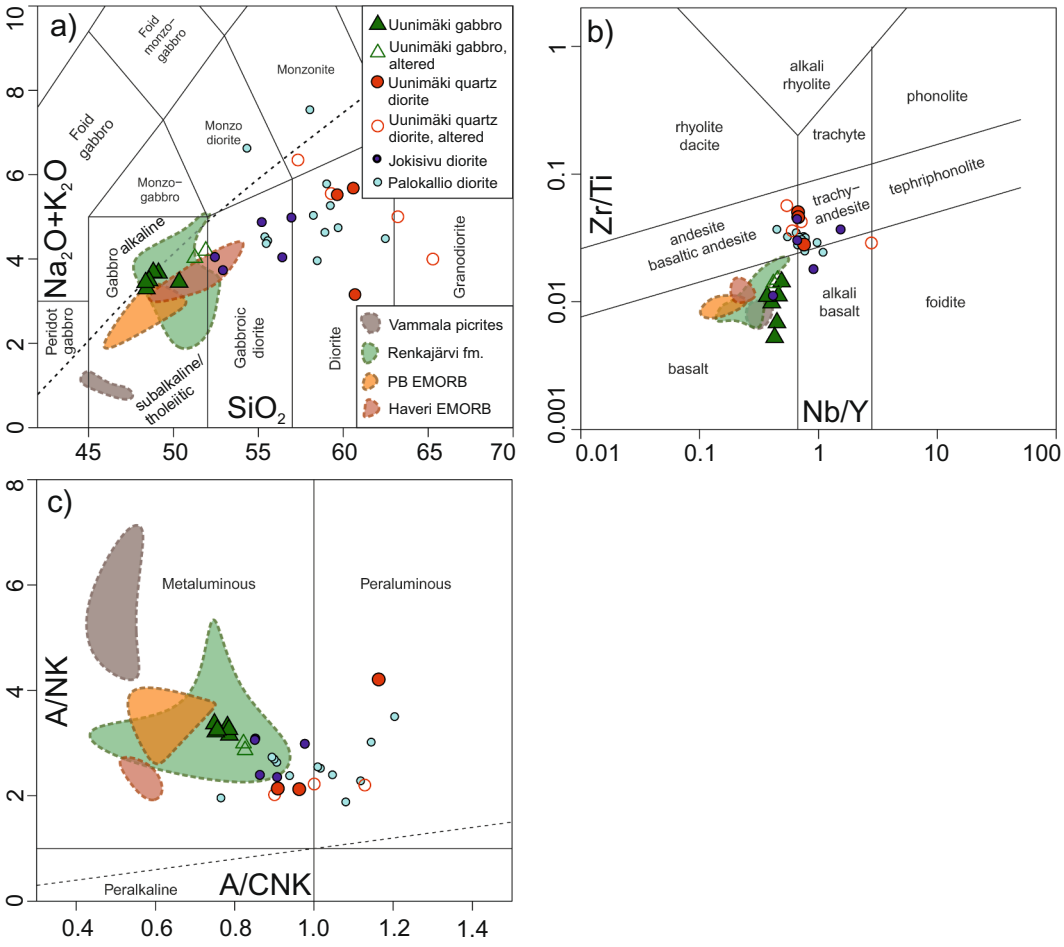

Fig. 6. Geochemical classification diagrams: a) total alkali vs. silica diagram (TAS; Middlemost, 1994), b) Zr/Ti vs. Nb/Y classification diagram (Pearce, 1996), c) Alumina saturation diagram (A/CNK vs. A/NK; Shand, 1943). Data for comparison are from Palokallio diorites (Voipio, 2008), Vammala picrites (Peltonen, 1995; Lahtinen et al., 2017), Renkajärvi suite (Sipilä and Kujala, 2014), Pirkanmaa belt (PB) (Sipilä and Kujala, 2014; Lahtinen et al., 2017) and Haveri E-MORBs (Strauss, 2004).

lack negative Nb-Ta anomaly but slight Zr-Hf anomaly can be observed in the multielement diagram (Fig. 7a). The REE-pattern of the UGB is gently sloping (Fig. 7b) with slight enrichment in LREE (La_N/Yb_N = 3.4–4.8; La_N/Sm_N = 1.6–2.4; Gd_N/Yb_N = 1.5–1.9). There are no Eu anomalies in the samples (Eu/Eu* = 0.89–1.14), but some variation in the total REE-content of the samples is visible (REE_{tot} = 71.4–103.4).

The quartz diorites are slightly enriched in the LILE elements with Rb contents of 48–128 ppm and Ba contents of 390–532 ppm. Sr contents are between 315 and 422 ppm. There is considerable variation in Ni and Cr contents, as these range between 3 and 42 ppm and 6 and 106 ppm, respectively. Two samples have anomalously low Ni and Cr contents (TALE-2017–12.1 and IJPI-2017–159.1), and sample TALE-2017–14.1 has anomalously high Ni and Cr contents. Nb content is between 10.9 and 17.4 ppm, except in sample TALE-2017–14.1, which has 42.9 ppm of Nb. Zr and Y contents are 167–241 ppm and 15–32 ppm, respectively. The samples show F contents between 442 and 485 ppm, except in sample TALE-2017–14.1, where it is 820 ppm. There is a weak negative Ta-Nb-anomaly and a significant negative Ti-anomaly in the samples. On the other hand, a very slight positive Zr-Hf-anomaly can be observed. The REE-slope of the quartz diorites and granodiorites is steeper than in the UGBs. The sample TALE-2017–12.1 is clearly anomalous as it is enriched in the HREE, so it is not included in the REE-calculations. The granodiorites and quartz diorites are enriched in LREE, but not in HREE (La_N/Yb_N = 4.8–12.6; La_N/Sm_N = 1.8–4.0; Gd_N/Yb_N = 1.4–2.0). There is no Eu anomaly.

In general, the Jokisivu and Palokallio samples show similar trace element characteristics to the quartz diorites. They show slight negative Ta-Nb anomaly and their Ti, Y and Yb values are below MORB. The REE-characteristics are similar to quartz diorites expect that the Palokallio samples show negative Eu-anomaly. The complete major and trace element data are available in Electronic Appendix B.

4.4. U-Pb zircon data

The UGB zircons are mostly elongated prismatic grains with length of 50–200 μm but only 15–55 μm in width (Fig. 8). This morphology is typical for zircon crystals in gabbros (Corfu et al., 2003). Their colour ranges from completely transparent to light brown. The inner structures of the zircon grains are very homogenous; few crystals show oscillatory zoning or cores and there are no visible inclusions. Cracks are common hampering to find large enough intact domains for spot analyses.

34 analyses were performed from 32 grains. Three different age populations were found from the analyses. a) An older population containing two zircons yielded $^{207}Pb/^{206}Pb$ ages of 1920 and 1917 Ma, but their U-Pb ages are between 1878 and 1826 Ma. b) The largest population contains 23 zircons and yielded a concordia age of 1891 ± 5 Ma. The $^{207}Pb/^{206}Pb$ age and an upper intercept age of the same zircons is 1895 ± 6 Ma (not shown). Five of these analyses show U-Pb ages between 1979 and 1902 Ma and plot slightly above concordia curve. One of the analyses show high ^{204}Pb. c) The youngest population consists of nine zircons and yielded $^{207}Pb/^{206}Pb$ ages between 1877 and 1835 Ma. All the analysed zircons show U/Th ratios between 0.37 and 0.55 and no textural differences can be recognized between the zircon populations. The concordia and $^{207}Pb/^{206}Pb$ weighted age diagrams are shown in Fig. 9. Full list of the U-Pb analyses are in Electronic Appendix D.

4.5. Lu-Hf zircon data

In general, the UGB zircon Hf isotopic compositions show chondritic values with a rather narrow range of five ε-units. A total of 16 analyses were performed on 16 grains and they exhibit initial $^{176}Hf/^{177}Hf$ values between 0.28149 and 0.28163 corresponding to initial ε_{Hf} values between −3.0 and 1.8 with an average value of −0.6 at 1892 Ma. The zircon Lu-Hf isotope data is compared to other relevant data of Fennoscandian shield in Fig. 10 and full list of the Lu-Hf analyses are in Electronic Appendix E.

5. Discussion

5.1. Age of the Uunimäki gabbro

The main zircon population yielded a concordia age of 1891 ± 5 Ma, which is the best estimate for the crystallisation age of the UGB. A weighted average $^{207}Pb/^{206}Pb$ age and an upper intercept age of the same grains yield slightly older, ~1895 Ma ages, but within errors they are similar. The origin of the older ~1.92 Ga zircons is unclear, but zircons with similar ages have been previously described in the Svecofennian domain (Huhma et al., 1991; Claesson et al., 1993; Lahtinen & Huhma, 1997; Rutland et al., 2004; Lahtinen et al., 2009b) and are therefore possibly inherited. They can also represent much older inherited grains which are isotopically incompletely reset during the 1.89 Ga event. The younger population of zircons, ~1.86 Ga and 1.84 Ga, could be interpreted to represent a later metamorphic or Pb-loss event. Approximately 1.87–1.86 Ga magmatism occurs in the region (Nironen, 1999; Kara et al., 2020) and younger magmatism is common further to the south, which potentially caused thermal effects on the studied rocks (e.g. Korsman et al., 1999). However, there is no difference in zircon morphology and Th/U ratios between the different age groups, which calls for an alternative explanation. The youngest zircons are high in common Pb (Electronic Appendix C), suggesting that these zircons did not remain isotopically closed system. Corfu (2013) showed that in single zircon analysis, with quite large error ellipsis, Pb-loss can apparently propagate along the concordia curve towards younger U-Pb

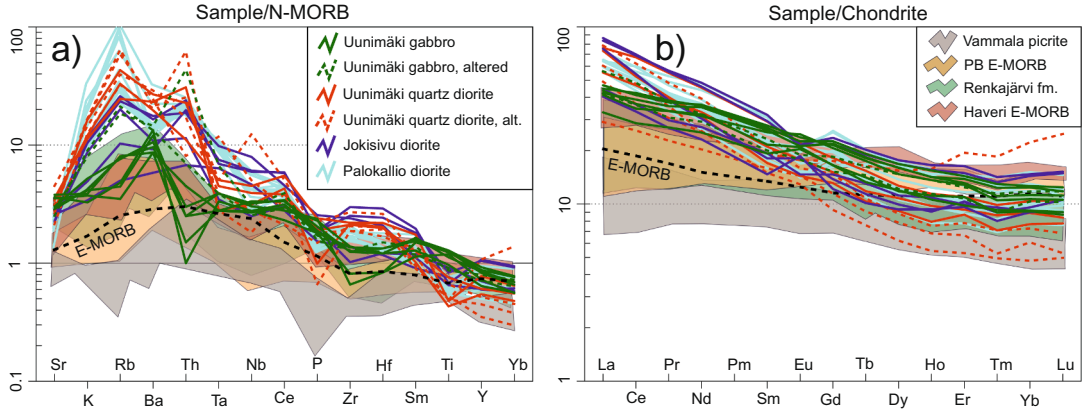

Fig. 7. a) Multielement diagram normalised to normal mid ocean ridge basalt (N-MORB; Pearce, 1983) and b) REE diagram normalized to C1 chondrite (Boynton, 1984). E-MORB reference pattern after Sun and McDonough (1989).

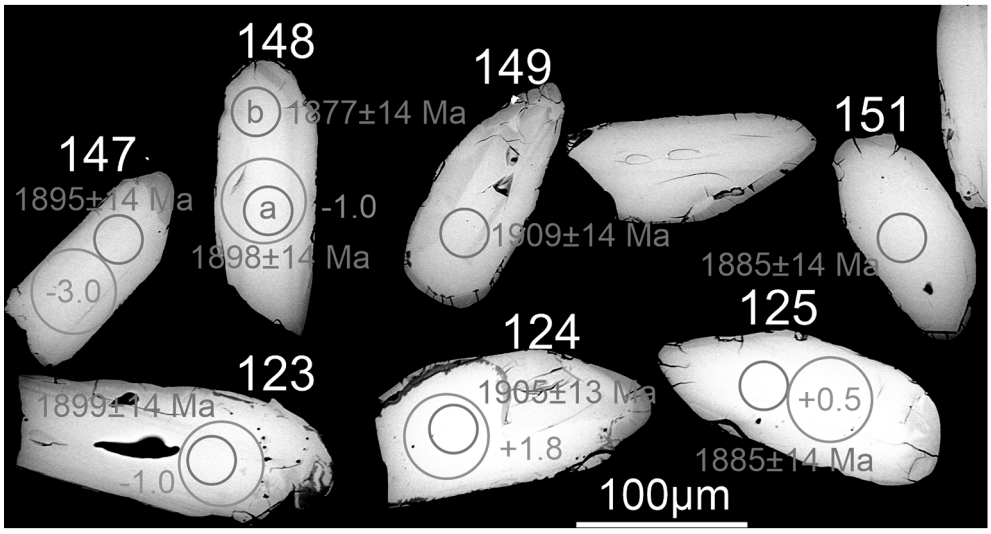

Fig. 8. Representative BSE-images of the zircons (TALE-2017–17.1). $^{207}Pb/^{206}Pb$ ages (in red, smaller spot) and initial ε_{Hf} values (in green, larger spot) indicated.

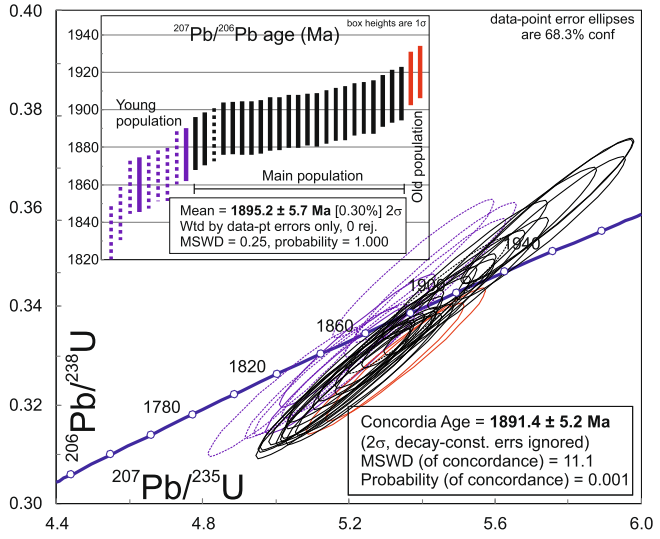

Fig. 9. U-Pb data for the analysed zircons. Analyses with high ^{204}Pb indicated by dashed line/ellipse.

ages if the event that caused the zircon crystal lattice rupture is not very much younger. Even though the gabbro sample selected for zircon separation was intact, the UGB was affected by shearing, faulting and fluid activity in many places, and these potentially affected the zircons. According to Saalmann et al. (2009, 2010) this late tectonic/fluid activity took place between 1.82 and 1.79 Ga. The Pb-loss model is supported also by the fact that the analyses show gradual decrease in $^{207}Pb/^{206}Pb$ ages.

The age relationship between the UGB and the quartz diorite is ambiguous since no direct cross-cutting relations were observed. The quartz diorite contains elongated MGEs, which are very common in igneous rocks (e.g., Paterson et al., 2004), but the source of the MGEs is unknown. A younger age is supported by the migmatitic paragneiss inclusion in the quartz diorite and the different geochemical features between the quartz diorite and the UGB (below). Therefore, we suggest that the quartz diorite is contemporaneous with the Jokisivu diorite (1884 ± 4 Ma; Saalman et al., 2010) and Nuutajärvi diorite (1881 ± 4 Ma; Kara et al., 2020) in the Pirkanmaa belt showing similar geochemical features. These intrusions are related to the regional upright folding (Kilpeläinen et al., 1998; Saalman et al., 2010) and are coeval with the peak metamorphism in the Pirkanmaa belt (Mouri et al., 1999). Moreover, the contrasting foliation patterns between the UGB and the quartz diorite (Section 4.2) likely reflect contrasting ages for these intrusive units.

The 1891 Ma of the UGB makes it the oldest dated igneous rock in the Häme belt. The Jokisivu diorite, hosting a gold deposit, is 5–10 Ma younger (Saalmann et al., 2010), although the ages overlap within errors. The older, pre-tectonic age for the UGB is supported by the spaced and localized deformation fabrics, whereas more penetrative foliations are characteristic for many of the *syn*-tectonic intrusions (Kilpeläinen, 1998). In general, the age determinations for synorogenic magmatism fall between ~1.88 and 1.87 Ga in the Häme belt (Patchett and Kouvo, 1986; Suominen, 1988; Nironen, 1999; Nironen, 2005; Saalmann et al., 2010; Mäkitie et al., 2016). By contrast, ≥ 1.89 Ga igneous ages dominate in the Pirkanmaa and Tampere belts (Kähkönen 2005; Lahtinen et al., 2017), which are considered to have coeval depositional and tectonic evolution (Lahtinen, 1994; Kilpeläinen, 1998; Kähkönen, 2005). The extension-related submarine Haveri formation lavas are interpreted to have erupted at 1.92–1.90 Ga (Kähkönen, 2005; Lahtinen et al., 2009b). However, the age is poorly defined and is based on stratigraphic relations (Kähkönen, 1999; Kähkönen, 2005) and whole rock Pb isotopes (Vaasjoki and Huhma, 1999). The following arc-type volcanism in the Tampere belt is bracketed between 1.90 and 1.89 Ga (Kähkönen, 2005), the Koskuenjärvi rhyolite being the oldest dated unit at 1904 ± 4 Ma (Kähkönen et al., 1989). Similar ~1.89 Ga ages have been interpreted for the tholeiitic small plutons within the Pirkanmaa belt (Peltonen, 2005). Moreover, the sedimentary rocks in both belts show maximum depositional ages between 1.92 and 1.89 Ga (Kähkönen, 2005; Lahtinen et al., 2009b; Lahtinen et al., 2017). These suggest that the UGB correlates to magmatism in the Pirkanmaa and Tampere belts rather than bulk of the Häme belt. Moreover, Lahtinen et al., (2017) considered that the stratigraphically lowermost sediments in the Häme belt within the Renkajärvi suite could be correlated to the Pirkanmaa belt sediments.

5.2. *Petrogenesis of the Uunimäki magmatic rocks*

All the analysed samples, even the altered ones, show low LOI contents (0.2–2.2 wt%) suggesting only weak post-magmatic alteration. The incompatible LILE and Ce, elements which are known to be mobile under medium-grade metamorphic conditions (e.g., Polat et al., 2002), record coherent compositions and correlate with immobile elements such as Zr (see Pearce and Cann, 1973) and the samples show Ce/Ce* ratios between 0.9 and 1.1 indicating limited LREE mobility.

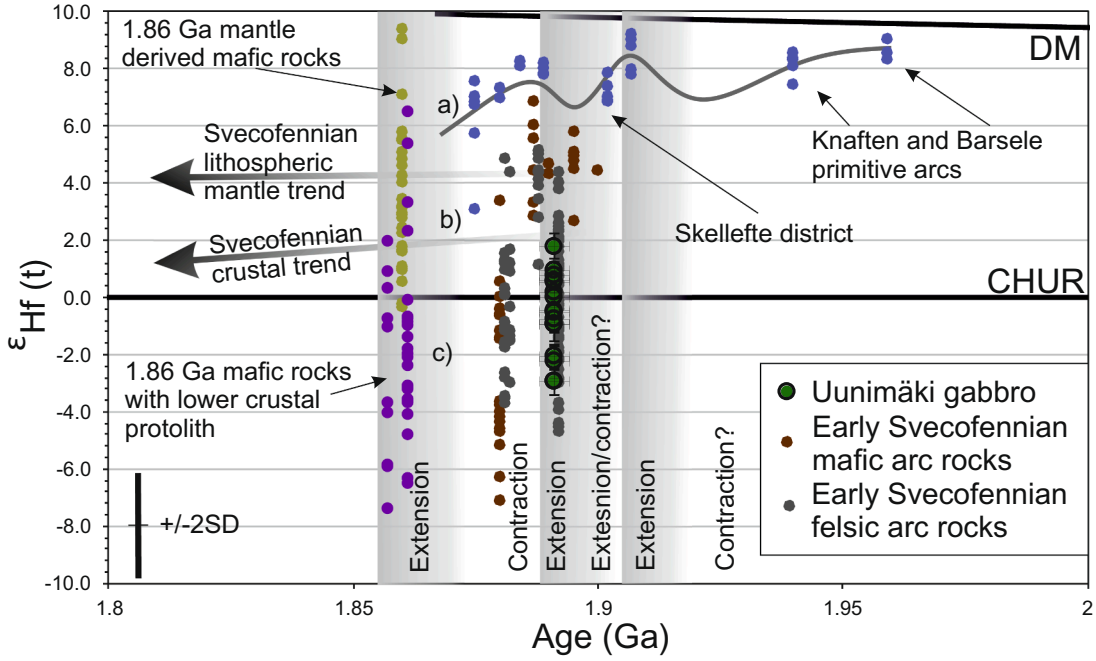

Fig. 10. $\varepsilon_{Hf\ (t)}$ vs. Age (Ga) diagram showing data from this study relevant reference data from the Svecofennian bedrock. CHUR = chondritic uniform reservoir (Bouvier et al., 2008); DM = depleted mantle (Griffin et al., 2000); Hf evolution trend for Svecofennian lithospheric mantle $\varepsilon_{Hf}(1.90)=+4.5 \pm 2.5$ and $^{176}Lu/^{177}Hf \approx 0.0315$ (Andersen et al., 2009, modified by Andersson et al. 2011); Hf evolution trend for the Svecofennian crust $\varepsilon_{Hf}(1.90)=+2 \pm 3$ and $^{176}Lu/^{177}Hf \approx 0.015$ (Andersen et al., 2009); blue dots (Barsele and Knaften arcs and Skelleftea district; Guitreau et al., 2014); Early Svecofennian mafic arc rocks (Patchett et al., 1982; Andersson et al., 2011; Kara et al., 2020); Early Svecofennian felsic arc rocks (Andersen et al., 2009; Heinonen et al., 2010; Andersson et al., 2011; Kara et al., 2018; Kara et al., 2020); yellow and purple dots (1.86 Ga mafic rocks; Kara et al., 2020). The grey line represents an approximation for Hf-time trend for the Skellefte area magmatism.

Petrographic studies confirm the primary nature of the samples (Fig. 5) and therefore trace elements, especially immobile elements, can be used for petrogenetic interpretations and to study the tectonic setting of the rocks.

The low MgO and Ni contents indicate that the tholeiitic parental magma for the UGB underwent fractional crystallisation of Mg-rich phases such as olivine and that the crystallising magma was rather evolved. The UGB shows clinopyroxene fractionation trends during the magma genesis based on correlation between MgO and $Fe_2O_3^T$ and CaO/Al_2O_3, Cr and V (Fig. 11a, b and c) and low Sc concentration. The small positive and negative Eu-anomalies (Eu/Eu* = 0.9–1.1) in separate samples suggest only minor fractionation/accumulation of plagioclase (Fig. 7). The negative correlation between mg# and V, TiO_2 and $Fe_2O_3^T$ (not shown) indicate late-stage Fe-Ti-oxide crystallisation in the magma and possible minor hornblende accumulation. Based on major elements the quartz diorites and the Palokallio and Jokisivu samples show similar but more evolved trends as the UGB. However, the trace element characteristics, e.g, negative Nb-Ta and Ti anomalies and positive Zr-Hf anomaly (Fig. 7) and Cr vs. V diagram (Fig. 11c) suggest that the UGB and the diorites have a different source and petrogenesis.

The role of crustal contamination during the UGB magma evolution is considered minor. Except slight LILE enrichment, this is suggested by the overall major and trace element characteristics, such as positive Nb-Ta anomaly and negative Zr-Hf anomaly (e.g., Rudnick and Gao, 2003; Fig. 7). Moreover, the narrow range of SiO_2 and the lack of correlation between SiO_2 and certain trace element ratios, which are used to trace crustal contamination, such as Nb/La, support this interpretation (Fig. 11d). The chondritic-like initial ε_{Hf} values might indicate crustal contribution but the rather small variation of 4.8 ε_{Hf} units supports a single source (Fig. 10). Considering the difficulty for the Hf isotopes to homogenise at a small scale (e.g. Griffin et al., 2002; Andersen et al., 2009), it is doubtful that this kind of Hf isotope homogeneity can be obtained by contamination of a mantle-derived magma by continental crust or by mixing mantle-derived and anatectic melt. However, these are the lowest ε_{Hf} values recorded from the early Svecofennian mafic rocks and are similar to the Svecofennian felsic arc magmas. In general, spatially extensive mildly depleted mantle source has been suggested for central Fennoscandia during the Paleoproterozoicum (e.g., Lahtinen and Huhma, 1997; Andersson et al., 2007; Rutanen et al., 2011; Kara et al., 2018). This feature is possible to explain by a more fertile mantle source for the UGB (below) containing unradiogenic Hf, i.e., older, recycled zircon-bearing crustal material ("zircon effect"; e.g., Patchett et al., 1984). The diorites show rather large spread in terms of LILE concentration and part of the samples are peraluminious (Fig. 6), which suggest some sedimentary assimilation during their genesis. The subduction component (e.g., Pearce and Peate, 1995), however, is apparent (Fig. 7) suggesting that the geochemical features reflect a subduction-related source rather than extensive upper crustal contamination. A hybrid nature is likely based on the MGEs.

Since crustal contamination for the UGB is regarded to be minor, several trace element ratios/diagrams indicate a mantle source similar to E-MORB-type rocks, i.e., enriched/fertile source and that the mafic magmas did not form by subduction (Pearce, 1996; Fig. 12a, b). LILE, especially Ba, and LREE are slightly more enriched compared to the average E-MORB but the pattern as well as the HFSE concentrations are similar (Fig. 7). The REE pattern is quite fractionated (La/Yb = 5.1–7) indicating that some residual garnet was left behind in the source. The samples fall between the garnet and spinel-garnet stability fields suggesting a small to moderate partial melting of garnet-spinel lherzolite of a source more enriched than the primitive mantle (Fig. 12d). Ratios of Zr/Ba (0.27–0.7; Menzies et al., 1991) and Nb/La vs. La/Yb diagram (Fig. 12c) show a mixed asthenospheric and lithospheric signature and a possible source for this type of signature could be the sub-continental lithospheric mantle (SCLM). This could also explain the small LILE enrichment (Fig. 7) and chondritic ε_{Hf} values (Fig. 10) since the SCLM is known to be chemically and isotopically heterogenous and can contain

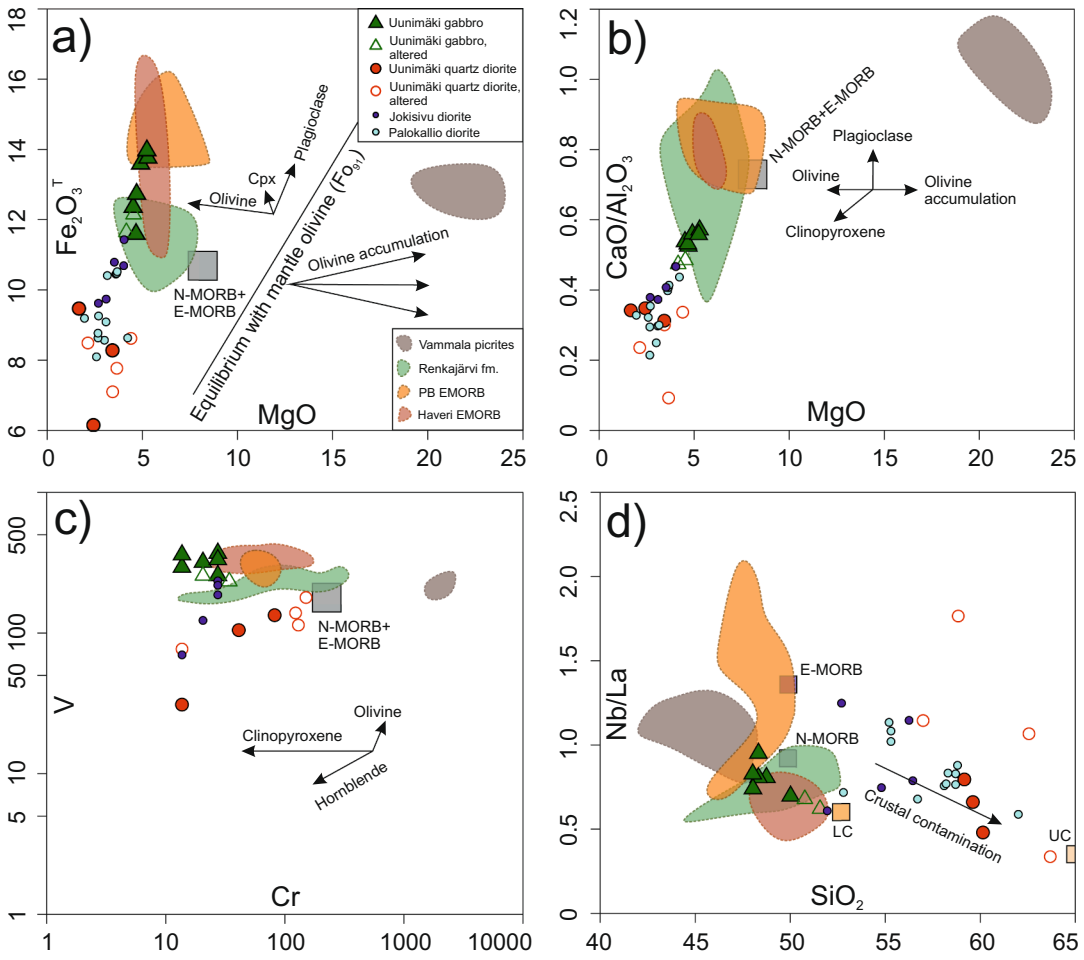

Fig. 11. Geochemical diagrams to estimate the role of fractional crystallisation (FC) (a-c) and assimilation-fractional crystallisation AFC (d) processes. N-MORB and E-MORB after Gale et al. (2013), lower crust (LC) and upper crust (UC) after Rudnick and Gao (2003). Equilibrium line of mantle olivine after Manikyamba et al., (2015). Schematic vectors on each diagram qualitatively indicate the relevant compositional effect of fractionation/accumulation of the indicated phenocryst phases (a-c) and effect of crustal contamination (d).

older zircon-bearing material (Pearson and Nowell, 2002). Moreover, lithospheric mantle is suggested to be present beneath the Central Finland Granitoid Complex and the Tampere belt at 1.91 Ga or earlier (Lahtinen & Huhma, 1997). According to the tectonic Zr-Nb-Th discrimination diagram, the UGB plot in E-MORB/within-plate tholeiitic field (Fig. 12e) indicating intra-continental environment. This conclusion can be further developed by Th-Nb-Ti vs. Yb diagrams (Fig. 12a, b), which points to a mature intra-oceanic, intra-continental back-arc or rifted margin setting. The quartz diorites and the Palokallio and Jokisivu samples do not plot neatly into the diagrams, but in average they show affinity to calc-alkaline arc-type rocks (Figs. 7 and 12). Similar setting has been proposed by numerous researchers for the ~1.88 Ga synorogenic magmatism (e.g., Nironen & Bateman, 1989; Lahtinen, 1996; Kähkönen, 2005).

5.3. *Geodynamic environment of E-MORB-type mafic rocks in Häme, Pirkanmaa and Tampere belts*

Since the UGB is E-MORB-like and differs from the Jokisivu and Palokallio diorites, we compare the UGB to the volcanic-plutonic rocks in Renkajärvi, Vammala, the Pirkanmaa belt and Haveri with reported E-MORB to MORB affinities (see Peltonen, 1995; Strauss, 2004; Sipilä & Kujala, 2014; Lahtinen et al., 2017). The UGB and the reference E-MORB rocks have nearly identical major element concentrations, their trace element compositions are similar and the multielement patterns have significant overlap (Fig. 7). The Vammala picrites are an exception as they show strong olivine accumulation (Fig. 11). The differences are only between single elements and the reference E-MORBs mostly show higher Th, Ni and Cr concentrations and, consequently, the multi-element pattern resembles the transitional basalts between the volcanic-arc and E-MORB/within-plate (VAB/WPB; Fig. 12a, e) settings as outlined by Pearce (1996). The subtle differences between the compared E-MORB rocks are best explained by different source characteristics and different level of partial melting. The Vammala picrites and the Pirkanmaa belt E-MORBs show the most depleted source characteristics in terms of several trace element ratios (e.g., Nb/La; Zr/Y; LREE/HREE) and show affinities to depleted MORB-mantle (DMM) type source (Fig. 12c, d and e). The Renkajärvi and Haveri samples show similarities to the UGB-type fertile SCLM source as also suggested by Lahtinen and Huhma (1997) for the Haveri, but higher level of partial melting is inferred (Fig. 12d).

The UGB and the Renkajärvi suite lie within the border zone between the Häme and Pirkanmaa belts. This spatial connection with similar geochemical features suggests a genetic link between the rocks. The geochemical features described above are uncharacteristic for subduction-induced magmatism (e.g., Pearce and Peate, 1995). Instead, they point to a rift-related environment, which indicate extensional tectonic regime (e.g., Xia & Li, 2019). Peltonen (1995) interpreted the Vammala picrites to represent an oceanic formation and Sipilä & Kujala (2014) noted that the Renkajärvi suite most likely formed by rifting, as opposed to other volcanic rocks in the Häme belt that have subduction-related geochemical affinities. Excluding the Haveri formation, we

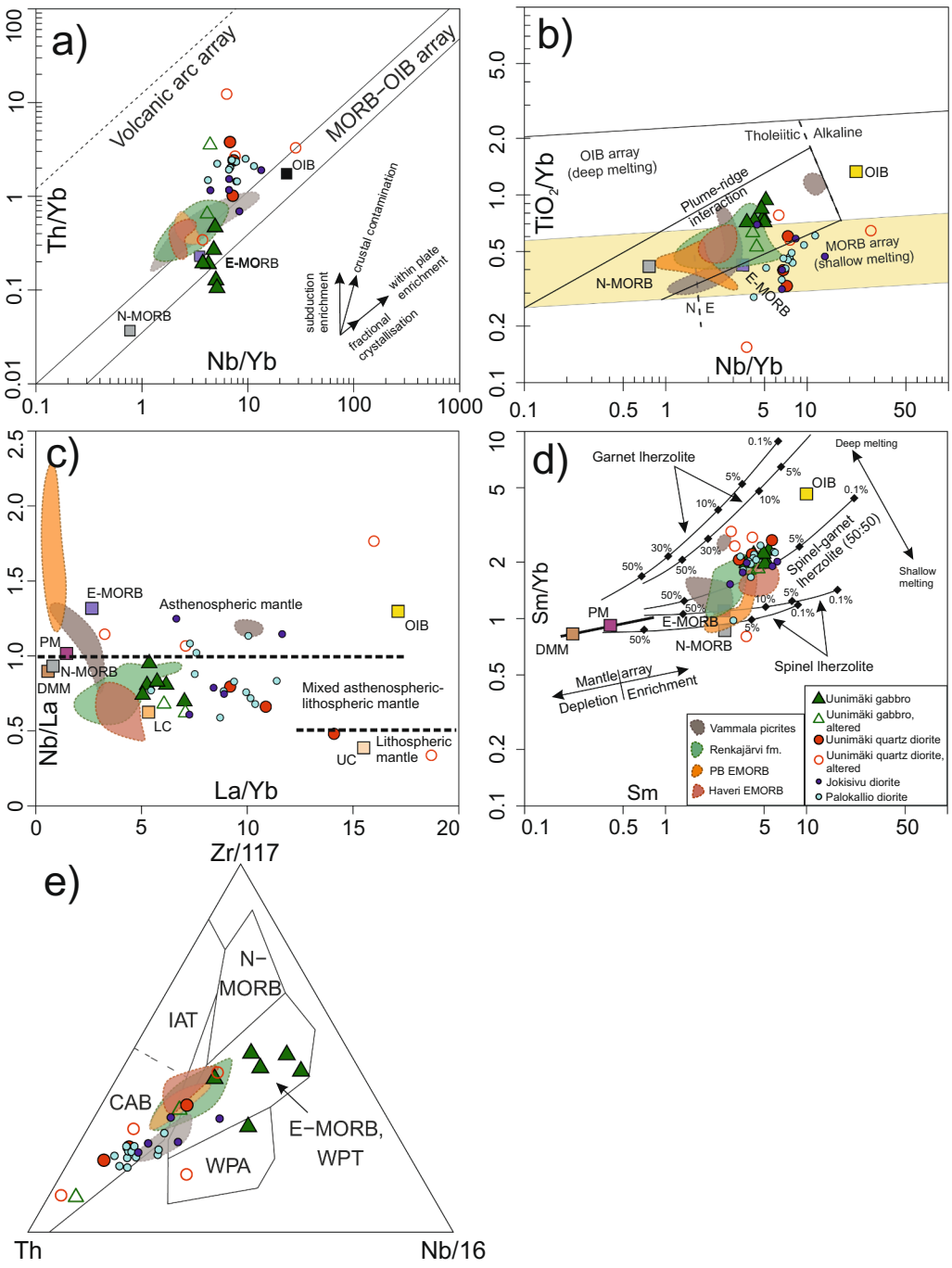

Fig. 12. Diagrams indicating mantle source, partial melting, subduction processes and geotectonic environment: a) Th/Yb vs. Nb/Yb diagram (Pearce, 2008), b) TiO_2/Yb vs. Nb/Yb diagram (Pearce, 2008), c) Nb/La vs. La/Yb diagram, fields for different mantle sources after Smith et al. (1999), d) Sm/Yb vs. Sm, partial melting curves for spinel, spinel-garnet and garnet lherzolite after Aldanmaz et al. (2000) and e) Th-Zr-Nb diagram (Wood et al., 1980). Depleted MORB-mantle (DMM; Salters and Stracke, 2004), primitive mantle (PM), N-MORB, E-MORB and OIB (Sun and McDonough, 1989), LC and UC (Rudnick and Gao, 2003).

suggest rifting in a previously formed (at ~1.92 Ga) fore-arc region for the tectonic setting of the E-MORB type rocks of this study in which the Tampere belt is the arc and the Pirkanmaa belt represents the fore-arc region (Fig. 13). The Vammala picrites and the Pirkanmaa E-MORBs are located slightly north off the UGB-Renkajärvi line but could represent a different rift of the same system. A more primitive geochemistry might indicate that the Vammala and Pirkanmaa E-MORBs were formed near the centre of a rift or represent more evolved rifting stage and thus have stronger contribution from DMM. The SCLM type source is proposed for the other E-MORB rocks. In this scenario the Haveri formation represents a back-arc environment of the Tampere belt (Strauss, 2004). This is plausible since the Tampere belt arc rocks show medium- to high-K characteristics indicating an evolved arc or continental margin setting (Kähkönen, 2005), suggesting that older > 1.91 Ga more primitive units, predating the Haveri formation, might exist. Lahtinen and Huhma (1997) suggested that SCLM layer evolved beneath continental nucleus (i.e., CFGC and the Tampere belt) surrounded by more juvenile island-arc accretions before 1.91 Ga. The SCLM trapped part of the fluids and small amounts of melts generating the enriched reservoir that was the source for the Haveri metalavas. Similar SCLM enrichment scenario is also consistent in the case of the UGB. Another explanation, based on uncertainties regarding the age, is that Haveri simply is younger, coeval with the UGB.

Rifting in a fore-arc region is favoured over a back-arc environment for the UGB due to a few reasons. Firstly, the magmatic rocks in the Häme belt are too young, ~1.88–1.87 Ga (Nironen, 1999; Kähkönen, 2005; Saalman et al., 2010; Mäkitie et al., 2016) for the Pirkanmaa belt to be a back-arc for the Häme belt. Secondly, southward dipping

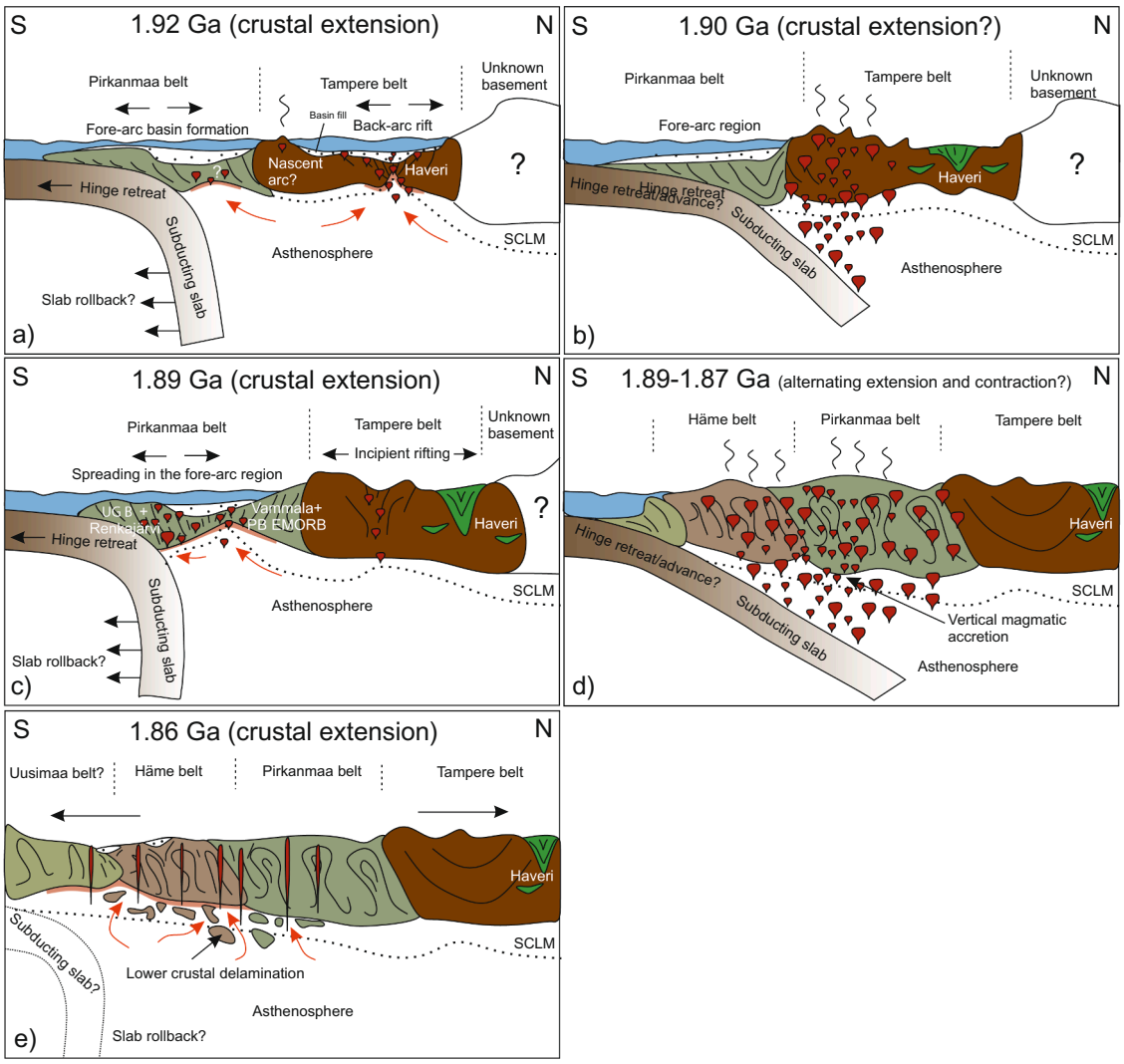

Fig. 13. Schematic N-S cross section of the magmatic evolution on the Tampere, Pirkanmaa and Häme belts at 1.92–1.86 Ga: a) extension, fore-arc formation and back-arc rifting of the nascent (?) Tampere arc; b) subduction related magmatism in the Tampere belt (during extension?); c) extension and rift-related magmatism in the forearc region of the Tampere belt; d) thrusting (and possible extension?) and subduction related magmatism in the Pirkanmaa and Häme belts; e) extension, lower crustal delamination and related within plate-type magmatism in the Häme, Pirkanmaa and Uusimaa belts. Not in scale, see text for discussion. SCLM = Sub continental lithospheric mantle.

subduction in north of the Tampere belt would be needed if the Pirkanmaa belt represents a back-arc environment of the Tampere belt and there is no evidence of such a subduction (e.g., Kähkönen, 2005; Chopin et al., 2020; Mints et al., 2020). Structural vergence, age constraints and overall tectonic models all support for the N-NE dipping subduction (Nironen et al., 2016; Hermansson et al., 2008; Chopin et al., 2020; Mints et al., 2020). A double-plunging subduction, opening and closure of a rift basin in the Pirkanmaa belt have also been suggested (e.g., Lahtinen et al., 2017; Nironen, 2017) but this is not entirely consistent with the age data of the Tampere and Häme belts nor with voluminous and rather long-lasting arc magmatism within both belts. Moreover, this model would imply obduction of ophiolites during the closure of ocean basin but, so far, indications of such formations have not been found. In our model, the reason for the extension is suggested to be a slab roll-back (Fig. 13; e.g., Wang et al., 2020). These would open a channel for mantle upwelling (e.g., Sternai et al., 2014; Cassel et al., 2018), which would cause rifting and the related magmatism within a fore-arc region.

Lahtinen et al., (2017) studied the stratigraphic evolution of SW Finland and also identified the rift-related environment using WPB-MORB volcanics, cherts and black shales as a “marker horizon”. They were able to extend the rift-related rocks to the Pohjanmaa belt (Fig. 1) and suggested an age of ~1.91 Ga based on sedimentary relations (see also Williams et al., 2008). This study now confirms the rift-related environment broadly at ~1.9 Ga. The obtained UGB age of ~1.89 Ga is considered as a minimum age for the rift-related magmatism. The maximum age of ~1.92 Ga is bracketed using the maximum depositional ages on related sedimentary rocks in Haveri and the Pirkanmaa belt (Kähkönen, 2005; Lahtinen et al., 2017). Whether the extensional tectonic regime prevailed continuously between 1.92 and 1.89 Ga or 1.92–1.90 Ga and 1.89 Ga are separate events would need more age determinations on structurally controlled samples. However, the rather well-documented arc-type magmatism between 1.90 and 1.89 Ga in the Tampere belt and the evidence of incipient rifting at ~1.89 Ga in the central Tampere belt (Kähkönen, 2005 and references therein) suggest that the different types of magmatism overlapped and might be related to prolonged extensional event (Rutland et al., 2004; Magni, 2019). The rift-related magmatism was shortly followed by crustal shortening, which is recorded by regional upright folding (e.g., Kilpeläinen, 1998; Saalmann et al., 2010; Chopin et al., 2020) and volcanic arc-type magmatism in the Häme and Pirkanmaa (and Pohjanmaa) belts at ~1.88 Ga. Our model supports the tectonic model of Hermansson et al. (2008) and Saalmann et al., (2009) with continuous subduction to N-NE beneath

single continental margin with constant polarity. The tectonic switching, i.e., the cyclic changes extension and short-lived (~10 Ma) contraction, results from hinge retreat and advance and is controlled by arrival of, e.g., buoyant oceanic plateaus at the trench (Collins, 2002a, 2002b). We infer that the rift-related magmas are related to the upper crustal extension while arc-type magmas can be related to either extension or contraction. However, when the arc-type magmas (or anatectic granites) are intruded into the axial planes of regional upright folds during crustal shortening event they can used to date the contractional phase. The dating of such events is therefore challenging but the main deformation with upright folding is dated approximately at 1.88 Ga in the Pirkanmaa and Pohjanmaa belts (Kilpeläinen, 1998; Rutland et al., 2004; Chopin et al., 2020) and between 1.88 and 1.87 Ga in the Häme and Tampere belts (Nironen, 1989; Nironen, 1999; Saalmann et al., 2010). Older thrusting events might exist, but they are still poorly constrained (Lahtinen et al., 2017). Based on the existing data, previously inferred stratigraphic evolution (Lahtinen et al., 2017) and the tectonic evolution (Kilpeläinen, 1998; Saalmann et al., 2010; Lahtinen et al., 2017; Chopin et al., 2020) we suggest the following evolution for the early Svecofennian magmatism in central Fennoscandia:

1.92–1.90 Ga: rift-related magmatism in the northern part of Tampere belt (Haveri) and possibly in the Pirkanmaa belt (crustal extension; Fig. 13a).

1.90–1.89 Ga: arc-type magmatism in the Tampere belt (crustal extension or contraction?; Fig. 13b).

1.89 Ga: rift-related magmatism within the Tampere belt fore-arc region, i.e., in the Pirkanmaa belt, in the northern part of the Häme belt and in the central Tampere belt (crustal extension; Fig. 13c).

1.89–1.87 Ga: arc-type magmatism in the Häme and Pirkanmaa belts (crustal thickening, alternating extension and contraction?; Fig. 13d).

~1.86 Ga: high-Nb and adakite-like, i.e., within plate-, type magmatism in the SW Finland (crustal extension; Fig. 13e, Kara et al., 2020).

Similar magmatic (and depositional) ages and rift-related magmatism to some extent continue through the Pohjanmaa belt (Williams et al., 2008; Lahtinen et al., 2017) to the Bothnia–Skellefte lithotectonic unit in northern Sweden (Fig. 1) where continued retreating subduction, extension, intra-arc basin development and sedimentation is suggested for tectonic evolution at 1.93–1.90 Ga. This was followed by advancing subduction-related magmatic activity at 1.88–1.87 Ga (Skyttä et al., 2020). Therefore, it is possible to continue the rift-related tectonic setting and suggested tectono-magmatic evolution further to the NW of our study area (see Lahtinen et al., 2017).

This model could explain the high temperature-low pressure (upper amphibolite to granulite facies) metamorphism within the Pirkanmaa belt at 1885–1880 Ma (Mouri et al., 1999; Lahtinen et al., 2017) by the thermal effect of asthenosphere upwelling, the mantle-derived magmatism and possible magmatic underplating due to lithosphere stretching (Fig. 13c; e.g., Collins, 2002a, 2002b). Chopin et al., (2020) noted also that the metamorphic mineral assemblages developed during the convergent episodes approximately at 1.89–1.88 Ga or 1.88–1.87 Ga within the Pohjanmaa belt. These observations are broadly in line with the model since Collins (2002a) suggested that peak metamorphic mineral assemblages crystallise during thrusting soon after the extensional event due to lithosphere cooling by isolating the crust from asthenosphere. In addition, indications of early metamorphism at ~1.92–1.91 Ga in the Pirkanmaa and Pohjanmaa belt metasediments is found in low Th/U zircon rims (Fig. 13a; Rutland et al., 2004; Williams et al., 2008; Lahtinen et al., 2017). The ~1.86 Ga extensional event is based on within-plate type gabbroic dykes and small intrusions in the Pirkanmaa, Häme and Uusimaa belts (Nevalainen et al., 2014; Kara et al., 2020) and opening of small rift-basins, now represented by lateritic paleosols and mature quartzites at the time or slightly later (Bergman et al., 2008; Lahtinen and Nironen, 2010). Recent identifications of ~1.86 Ga metamorphic event in southern Finland (Väisänen et al., 2021; Vehkamäki et al., 2021) might indicate lithospheric thinning (i.e., extension; Collins, 2002b). However, the tectonic framework of this event is still poorly constrained (Torvela and Kurhila, 2020). Kara et al., (2020) suggested that the 1.86 Ga magmatism in linked to lower crustal delamination (Fig. 13e) but whether this delamination is the consequence or the reason for the extension is ambiguous. Delamination driven extension (cycle) in the absence of slab rollback is interpreted in the Sevier-Laramide orogen in the western U.S. (Wells et al., 2012). Also, other drivers for crustal extension have been proposed at ~1.86 Ga, such as distributed thickening-induced lateral flow (Cagnard et al., 2007), accretion followed by gravitational spreading (Nikkilä et al., 2015) and far-field plate motions and orogenic collapse (Lahtinen et al., 2005). We consider that the lower crustal delamination (Kara et al., 2020) with or without slab rollback would provide the most comprehensive model. The above-mentioned occurrences suggest a north to south "zonation" of the metamorphism at ~1.92 Ga, 1.89–1.88 Ga and ~1.86 Ga in SW Finland coupled with extensional phases in the developing arc-system. Unfortunately, the metamorphic events at ~1.92 Ga in the Pirkanmaa belt (e.g., Rutland et al., 2004) and at ~1.86 Ga in the Häme and Uusimaa belts (e.g., Väisänen et al., 2021) are largely overprinted by later regional metamorphism, 1.89–1.88 Ga event in the north and 1.83–1.82 Ga event in the south making their characterisation difficult. Nevertheless, we suggest that the driver for the ~1.92 Ga, 1.89–1.88 Ga and ~1.86 Ga metamorphisms is the lithosphere thinning coupled with mantle-derived magmatism and lower crustal delamination (at 1.86 Ga) due to extension rather than thrusting and crustal thickening. However, during later regional metamorphism at 1.83–1.82 Ga in southern Finland crustal thickening and radioactive heat production (Kukkonen and Lauri, 2009) should be considered.

The fate of the active subduction is obscure after ~1.87 Ga, since clear arc-type rocks are not found after that time in southern Finland (e.g., Lahtinen and Nironen, 2010). Several possible explanations exist: (i) subduction zone migration further to the SW (Saalmann et al., 2009), (ii) continent–continent collision (Lahtinen et al., 2005), (iii) accretion of another arc-system, i.e., the Uusimaa belt against the Häme, Pirkanmaa and Tampere belts, relocating the subduction zone further to SW. Whether the Uusimaa belt share the same geological history as the other belts is obscure due to some older magmatic ages found within the Uusimaa belt compared to the belts in the north (e.g., Väisänen & Mänttäri, 2002; Kara et al., 2018). Korja et al. (2006) regarded the Häme and Uusimaa belts as separate terranes, whereas Väisänen and Mänttäri (2002) suggested that the belts belonged to the same arc system but were rifted apart. The Uusimaa belt also contains E-MORB- (Väisänen & Mänttäri, 2002) to transitional MORB-type rocks (Väisänen and Westerlund, 2007) but whether these can be correlated to the same tectonic switching cycle would need more age determinations. Another open question is that whether the evolution of the Tampere, Pirkanmaa and Häme belts can be correlated with the suggested cyclic geodynamic evolution of the south-central Sweden (Hermansson et al., 2008) or are these separate arcs? Considering these aspects, it is possible that the Uusimaa belt was formed in the same arc system as the south-central Sweden (Hermansson et al., 2008; Saalmann et al., 2009), which was accreted against the Tampere, Pirkanmaa and Häme belts.

5.4. Implications for crust generation

The tectonic switching model generally involves formation of repeated back-arc basins (Collins, 2002a, 2002b) and therefore our model with extension in the previously formed fore-arc region is not conventional. However, modern analogues of such settings can be found, for example, from the Zagros belt in NE Iraq and SW Iran where gabbros with composition similar to the UGB erupt and crosscut the 20 m.y.r. earlier formed fore-arc due to extension (Ao et al., 2016; Al Humadi et al., 2019; Moghadam et al., 2020) as well as in the Banda arc system in eastern Indonesia in which slab roll-back is suggested to drive extension in the fore-arc environment (Pownall et al., 2016). Rift-related environments within fore-arcs are also identified in the vast Central Asian Orogenic Belt (e.g., Windley et al., 2007). Moreover, in the

Devonian–Carboniferous New England Orogen, eastern Australia, McKibbin et al., (2017) suggested a fore-arc-arc-back-arc setting, broadly similar as described here, developed by tectonic switching cycle. This setting also contains tholeiitic gabbro bodies similar to the UGB with inferred fore-arc affinities (McKibbin et al., 2017). The New England orogen is considered as outboard extension of the Lachlan orogenic belt, which is the prime example of the model (Collins, 2002a, b). These examples suggest that fore-arc environments can be in notable position in the tectonic switching cycle.

At the present erosional level, the rift-related magmatic rocks comprise < 5 % of the total area of the bedrock in SW Finland and therefore, volumetrically their role can be considered minor. However, the overall role of extensional tectonic regime can be considered essential for the crust generation during an accretionary orogen (Collins, 2002a, b). Although the record is incomplete, zircon Hf isotope coupled with whole rock Nd isotope data allow us to evaluate the additions of mantle-derived material to the crust (Kemp et al., 2009) during the early stages of the Svecofennian orogen and, more broadly, during different tectonic cycles in accretionary Paleoproterozoic orogens. Two types of mafic magmatism seem to prevail during the rifting: primitive magmas and magmas with recycled crustal component. The Vammala picrites and Pirkanmaa E-MORB are representatives for primitive magmas based on depleted $_{\varepsilon Nd}$ values and primitive geochemistry, whereas the UGB, Haveri and Renkajärvi rocks show more extensive recycled crustal component based on chondritic zircon $_{\varepsilon Hf}$ values (UGB), $_{\varepsilon Nd}$ values (Haveri) and enriched geochemistry. Similar rocks from both groups seem to continue to the Pohjanmaa belt (Lahtinen et al., 2017). The primitive magmas represent almost completely juvenile additions to the crust, whereas our approximation infers that the juvenile component is approximately 85 % for the UGB-type enriched rocks (see Electronic Appendix A for the details of the calculation). Therefore, the magmatic influx to the crust was mostly juvenile during the rift-related magmatism. The zircon Hf isotope-time trends follow the extension-contraction cycle to some extent by showing stronger crustal contribution during or after the thickening events (e.g., ~1.88 Ga) in the arc magmatism (Kemp et al., 2009; Fig. 11). The trend is most pronounced in the oldest juvenile units, the Knaften and Barsele (and Savo, only Sm-Nd data) primitive arcs (Lahtinen & Huhma, 1997; Guitreau et al., 2014; Fig. 1) and crustal recycling gradually increases with time in the Skellefte district (Fig. 11). During the extensional events the juvenile magmatism would be expected due to lithosphere thinning but the isotope trend is twofold as mentioned above: some units like the Vammala picrites are very juvenile while other, like the UGB, show some crustal contribution. This can be explained by different mantle source characteristics (SCLM vs. asthenosphere) and possibly by the distance to the active subduction zone. The different source characteristics also applies to the later extension-related 1.86 Ga mafic magmas, which show very different Hf-isotope features depending on the source (Fig. 11; Kara et al., 2020). The recycling processes are arguably more notable during the voluminous bimodal magmatism within or after the shortening events, which is recorded by low $_{\varepsilon Hf}$ values. Besides the recycling processes, this magmatism provides magmatic vertical accretion (e.g., Cawood et al., 2009).

Another, perhaps more important aspect, is the possible basaltic underplating formed during the extensional phases of the Svecofennian orogeny (Stephens and Andersson, 2015), which can be interred from the seismic profiles from the Tampere and Pirkanmaa belts (Lahtinen et al., 2009a). Similar pulses of mafic underplating are inferred from Bergslagen (Stephens & Andersson, 2015) and the SW Svecofennian domain in Sweden (Andersen, et al., 2009). These represent significant fluxes from the mantle to the lower crust (e.g., Davidson and Arculus, 2006) but characterising the exact nature and age components of the mafic underplating is difficult. Besides the crustal processes, formation of the Proterozoic SCLM during extensional environments by ~10% melt extraction has been suggested (Griffin, et al., 1999). As mentioned, the SCLM was present beneath the Tampere belt at 1.92 Ga (Lahtinen and Huhma, 1997) and beneath the Pirkanmaa belt at 1.89 Ga.

The period around 1.9 Ga is recognised as one of the major juvenile crustal growth episodes, which is linked to the supercontinent cycle (e.g., Stein and Hofmann, 1994). The reason for the episodic nature of the growth, however, remains debatable (e.g., Condie, 1998). Kemp et al. (2009) suggested that crustal growth could be explained simply by subduction and slab retreat, i.e., by alternating extensional and contractional tectonic regimes using the Australian Tasmanides, as a Phanerozoic example. Indeed, the early Svecofennian tectonic switching cycle at 1.92–1.86 Ga (Hermansson et al., 2008) represents a period of very rapid crust generation and substantial additions of juvenile mantle material to the crust. The Svecofennian orogen covers an area of ~1 million km^2 (Lahtinen et al., 2009a) and roughly 50–70 % of it was formed during the early 50 m.y. period. This with other almost coeval Paleoproterozoic examples from the Trans-Hudson orogen in Canada (e.g., Hollings and Ansdell, 2002), possibly the Usagaran belt in Tanzania (Bahame et al., 2016) and Tapajós Gold Province in Brazil (Lamarão et al., 2002) suggest that the tectonic switching might be significant driver for the ancient crustal growth pulses.

5.5. Geological controls of gold the mineralisation

Gold within the UGB was precipitated into the north-eastern part of the intrusion, which is characterised by the NW-NE trending high-strain zones. However, only one of the four most significant Au-rich intersections within the SW-plunging drillholes may be directly correlated with high-strain zones recognised in this study (Fig. 3b; R25 at measured depth, MD 46–48 m; 88–91 m; 97–106 m), whereas the three other (R8 at MD 7–15 m; 41–42 m, 52–53 m + R23 at MD 23.8–24.8 m + R314 at MD 39.3–40.3 m; 64.5–65.5 m; 82.5–84.5 m) occur at the margin of the high and low-strain domains. Consequently, the distribution of the Au-rich drillhole intersections is in line with Kärkkäinen et al. (2016) in that gold is not within the shear zone itself, which have acted as major fluid channel, but in the small quartz and pyrrhotite veins in the wall rock close to the sheared and altered zones. Placed within the context of the structural interpretation presented in Fig. 3b, we attribute the precipitation of gold to deformation zones representing 3rd and 4th order structures (based on zone length and inferred abutting relations; in line with Saalmann et al., 2009): the Kankaanranta SZ is the 1st order structure allowing the fluid flow from depth. The Helmelä SZ, interconnected to the Kankaanranta SZ, is the 2nd order structure, and allowed further fluid transport to the UGB. The 3rd order structures are represented by high-strain zones parallel to the Helmelä SZ, and these host part, likely the minority, of the gold mineralisations. The majority of mineralisations are located within the 4th order fracture networks occurring outside the high-strain zones, but kinematically likely linked to them.

The role of the Kankaanranta SZ as the main fluid pathway for gold-bearing fluids for the Uunimäki mineralisation is supported by its transpressional character, which suggests a correlation with the regional 1.83–1.79 Ga E-W shear zones of southern Finland (Väisänen and Skyttä, 2007). Moreover, the above timing is compatible with the 1.83–1.79 Ga timing of late-orogenic and the late-orogenic WNW-ESE transpression and gold-precipitating fluid movement in the western Häme belt (Saalmann et al., 2009) and also indicates that the gold mineralisation in the UGB is contemporaneous with the Jokisivu deposit (Saalmann et al., 2010). Saalmann et al. (2009) highlighted the pronounced regional NW-SE alignment of gold occurrences in southern Finland, and the UGB mineralization apparently is one member within this system. As the structural grain of the UGB mineralisation also trends NW-SE, we further attribute the ore-forming fluid flow to the NW-SW orientation of the Helmelä SZ and the parallel high-strain zones transecting the UGB, which were dominantly subjected to opening-mode stresses during the late-orogenic transpression.

The gold precipitated most likely in several stages, indicated by several vein generations (Fig. 4a-e; Kärkkäinen et al., 2016) and occurrence of large and complex gold grains with variable chemical

compositions (Fig. 4f-h; Kärkkäinen et al., 2015). The hydrothermal processes have probably been active in semi-ductile environment at mesozonal depths (6–12 km) indicated by breakdown of pyroxene and magnetite to hornblende but also clinopyroxene crystallisation in Au- and Bi-bearing metamorphosed quartz-carbonate vein (Fig. 4d; Kärkkäinen et al., 2016), As-enrichment (Groves et al., 1998) and deformation in conditions near the brittle-ductile-boundary (Leskelä, 2019). However, the silicate-sulfide veins formed in a semi-ductile environment are crosscut by sericite-rich veins and seams (Fig. 4b, d) that developed mainly in a brittle environment (Kärkkäinen et al., 2016) indicating that the fluid-activity continued in brittle environment. Also, part of quartz veins was formed in brittle environment (Fig. 2b) of which some contain native gold (Fig. 4f).

The hosting rocks for the Uunimäki, Palokallio and Jokisivu mineralisations have different geochemical signatures and different ages. Consequently, it is the structure and not the geochemical features or the age of the gold-hosting rocks, which provided the primary control over gold precipitation within the western Häme belt. However, the hosting intrusive rocks must have had a distinct mechanical contrast to the surrounding country rock so that the required 3rd – 4th order structures developed. The structural control for orogenic gold deposits has been widely recognized (e.g. Goldfarb et al., 2005), and the control may be simple such as the veining at dilational sites (Cox et al., 1995), or more complex, including e.g. inheritance of gneissic banding (Blenkinsop and Doyle, 2014) and other compressional structures (Upton and Craw, 2014), or host rock variation causing variation in the geometry of the ore-hosting fault, and the ore grade (Bell et al., 2017). The required mechanical contrast is evident for the diorites and gabbros hosting the Jokisivu, Palokallio and Uunimäki deposits, but here we further claim the variation in chemical composition between the sites may play a role in the style of the mineralisation: gold in the Jokisivu and Palokallio deposits is enriched in the quartz veins in the shear zones, whereas in Uunimäki the gold is not within the shear zone itself, but in the small quartz and pyrrhotite veins in the wall rock next to the high-strain zones. We infer this relates to the more basic and iron rich composition of the UGB which promotes sulphide precipitation during the fluid movement. Consequently, the tectonic setting of the host-rock does not directly play an important role in the gold precipitation, but the chemical composition, especially the iron composition, depends on the tectonic setting. These observations can be applied more widely in orogenic gold exploration in deformed Precambrian terrains. As a rule of thumb, the following might be used as a proxy for gold: (i) mechanical contrast between the host-rock and country-rocks, i.e., mafic intrusive vs. metamorphosed supracrustal rocks, (ii) 3rd – 4th order structures nearby the larger regional shear zones. Moreover, the chemical contrast between the host-rock and country-rocks may define the character of mineralisation.

6. Conclusions

- The 1891 ± 5 Ma age of the Uunimäki gabbro makes it the oldest dated plutonic rock in the Häme belt. The Au-bearing Jokisivu diorite in the same area is ~10 Ma younger.
- The E-MORB type geochemical affinity of the UGB points to rift-related setting in contrast to the Au-bearing Jokisivu and Palokallio diorites, which show arc-type signatures. It resembles the E-MORB-type volcanic rocks in SW Finland, closest the Renkajärvi, Haveri and Pirkanmaa belt volcanics.
- Rifting in a fore-arc region within a north-dipping subduction system is suggested for the tectonic environment. Slab retreat due to roll-back is suggested to cause the extension and related magmatism.
- Rapid crust generation, alternating rift-related and arc-type magmatism, extension-driven metamorphism and formation of the SCLM is suggested during the tectonic switching cycle of the early Svecofennian orogeny.
- The gold mineralisation in the Uunimäki gabbro was precipitated into fracture networks within the immediate vicinity of the NW-SE high-strain zones characterising the north-eastern high-strain domain of the intrusion.
- The ENE-WSW transpressional Kankaanranta shear zone, with structural linkage to the UGB, was likely the primary pathway for mineralising fluids.
- The geochemical details, the age of emplacement and the tectonic setting have therefore not played a major role in gold precipitation in the studied mafic rocks.

CRediT authorship contribution statement

Jaakko Kara: Conceptualization, Project administration, Funding acquisition, Investigation, Visualization, Writing – original draft. **Tuomas Leskelä:** Investigation, Writing – original draft. **Markku Väisänen:** Conceptualization, Funding acquisition, Writing – original draft, Supervision. **Pietari Skyttä:** Conceptualization, Funding acquisition, Writing – original draft, Supervision, Visualization. **Yann Lahaye:** Investigation, Methodology. **Markku Tiainen:** Investigation, Resources, Funding acquisition. **Hanna Leväniemi:** Investigation.

Declaration of Competing Interest

The authors declare that they have no known competing financial interests or personal relationships that could have appeared to influence the work reported in this paper.

Acknowledgements

This study was funded by the Geological Survey of Finland through the collaborative TYTY-project and by J. Kara's personal grant from The Finnish Cultural Foundation. Niklas Tenovuo prepared the thin sections, Arto Peltola the zircon mount and Matti Vuorisalo helped with zircon separation. Dragon Mining Oy is thanked for providing drill core samples from the Jokisivu diorite. We acknowledge Niilo Kärkkäinen and GTK for permission to use the photographs in Fig. 4.

Appendix A. Supplementary data

Supplementary data to this article can be found online at https://doi.org/10.1016/j.precamres.2021.106364.

References

Aldanmaz, E., Pearce, J.A., Thirlwall, M.F., Mitchell, J.G., 2000. Petrogenetic evolution of late Cenozoic, post-collision volcanism in western Anatolia, Turkey. J. Volcanol. Geoth. Res. 102, 67–95. https://doi.org/10.1016/S0377-0273(00)00182-7.

Al Humadi, H., Väisänen, M., Ismail, S.A., Kara, J., O'Brien, H., Lahaye, Y., Lehtonen, M., 2019. U-Pb geochronology and Hf isotope data from the Late Cretaceous Mawat ophiolite. NE Iraq. Heliyon 5, e02721. https://doi.org/10.1016/j.heliyon.2019.e02721.

Andersen, T., Andersson, U.B., Graham, S., Åberg, G., Simonsen, S.L., 2009. Granitic magmatism by melting of juvenile continental crust: new constraints on the source of Palaeoproterozoic granitoids in Fennoscandia from Hf isotopes in zircon. J. Geol. Soc. 166, 233–247. https://doi.org/10.1144/0016-76492007-166.

Andersson, U.B., Rutanen, H., Johansson, Å., Mansfeld, J., Rimša, A., 2007. Characterization of the Paleoproterozoic mantle beneath the Fennoscandian Shield: Geochemistry and isotope geology (Nd, Sr) of~ 1.8 Ga mafic plutonic rocks from the Transscandinavian Igneous Belt in southeast Sweden. Int. Geol. Rev. 49, 587–625. https://doi.org/10.2747/0020-6814.49.7.587.

Andersson, U.B., Begg, G.C., Griffin, W.L., Högdahl, K., 2011. Ancient and juvenile components in the continental crust and mantle: Hf isotopes in zircon from Svecofennian magmatic rocks and rapakivi granites in Sweden. Lithosphere 3, 409–419. https://doi.org/10.1130/L162.1.

Ao, S., Xiao, W., Jafari, M.K., Talebian, M., Chen, L., Wan, B., Ji, W., Zhang, Z., 2016. U-Pb zircon ages, field geology and geochemistry of the Kermanshah ophiolite (Iran): from continental rifting at 79 Ma to oceanic core complex at ca. 36 Ma in the southern Neo-Tethys. Gondwana Res. 31, 305–318. https://doi.org/10.1016/j.gr.2015.01.014.

Bahame, G., Manya, S., Maboko, M.A., 2016. Age and geochemistry of coeval felsic volcanism and plutonism in the Palaeoproterozoic Ndembera Group of southwestern

Tanzania: Constraints from SHRIMP U-Pb zircon and Sm–Nd data. Precambr. Res. 272, 115–132. https://doi.org/10.1016/j.precamres.2015.10.017.
Bedrock of Finland – DigiKP. Digital map database [electronic resource]. Espoo: Geological Survey of Finland [referred 1.10.2020] Version 2.1.
Bell, R.M., Kolb, J., Waight, T.E., 2017. Assessment of lithological, geochemical and structural controls on gold distribution in the Nalunaq gold deposit, South Greenland using three-dimensional implicit modelling. Geol. Soc. Spec. Pub. 453, 385–405. https://doi.org/10.1144/SP453.2.
Bergman, S., Högdahl, K., Nironen, M., Ogenhall, E., Sjöström, H., Lundqvist, L., Lahtinen, R., 2008. Timing of Palaeoproterozoic intra-orogenic sedimentation in the central Fennoscandian Shield; evidence from detrital zircon in metasandstone. Precambr. Res. 161, 231–249. https://doi.org/10.1016/j.precamres.2007.08.007.
Blenkinsop, T.G., Doyle, M.G., 2014. Structural controls on gold mineralization on the margin of the Yilgarn craton, Albany–Fraser orogen: The Tropicana deposit, Western Australia. Journal of Structural Geology 67, 189–204. https://doi.org/10.1016/j.jsg.2014.01.013.
Bogdanova, S., Gorbatschev, R., Skridlaite, G., Soesoo, A., Taran, L., Kurlovich, D., 2015. Trans-Baltic Palaeoproterozoic correlations towards the reconstruction of supercontinent Columbia/Nuna. Precambr. Res. 259, 5–33. https://doi.org/10.1016/j.precamres.2014.11.023.
Bouvier, A., Vervoort, J.D., Patchett, P.J., 2008. The Lu–Hf and Sm–Nd isotopic composition of CHUR: constraints from unequilibrated chondrites and implications for the bulk composition of terrestrial planets. Earth Planet. Sci. Lett. 273, 48–57. https://doi.org/10.1016/j.epsl.2008.06.010.
Boynton, W.V., 1984. Cosmochemistry of the rare earth elements: meteorite studies. Developments in Geochemistry 2, 63–114. https://doi.org/10.1016/B978-0-444-42148-7.50008-3.
Cagnard, F., Gapais, D., Barbey, P., 2007. Collision tectonics involving juvenile crust: the example of the southern Finnish Svecofennides. Precambr. Res. 154, 125–141. https://doi.org/10.1016/j.precamres.2006.12.011.
Cassel, E.J., Smith, M.E., Jicha, B.R., 2018. The impact of slab rollback on earth's surface: uplift and extension in the hinterland of the North American Cordillera. Geophys. Res. Lett. 45, 10–996. https://doi.org/10.1029/2018GL079887.
Cawood, P.A., Kröner, A., Collins, W.J., Kusky, T.M., Mooney, W.D., Windley, B.F., 2009. Accretionary orogens through Earth history. Geol. Soc., London, Spec. Publ. 318, 1–36. https://doi.org/10.1144/SP318.1.
Chopin, F., Korja, A., Nikkilä, K., Hölttä, P., Korja, T., Abdel Zaher, M., Kurhila, M., Eklund, O., Rämö, O.T., 2020. The Vaasa Migmatitic Complex (Svecofennian Orogen, Finland): Buildup of a LP-HT Dome During Nuna Assembly. Tectonics 39, e2019TC005583. 10.1029/2019TC005583.
Claesson, S., Huhma, H., Kinny, P.D., Williams, I.S., 1993. Svecofennian detrital zircon ages—implications for the Precambrian evolution of the Baltic Shield. Precambr. Res. 64, 109–130. https://doi.org/10.1016/0301-9268(93)90071-9.
Collins, W.J., 2002a. Hot orogens, tectonic switching, and creation of continental crust. Geology 30, 535–538. https://doi.org/10.1130/0091-7613(2002)030<0535:HOTSAC>2.0.CO;2.
Collins, W.J., 2002b. Nature of extensional accretionary orogens. Tectonics 21, 6–11. https://doi.org/10.1029/2000TC001272.
Condie, K.C., 1998. Episodic continental growth and supercontinents: a mantle avalanche connection? Earth Planet. Sci. Lett. 163, 97–108. https://doi.org/10.1016/S0012-821X(98)00178-2.
Corfu, F., Hanchar, J.M., Hoskin, P., Kinny, P., 2003. Atlas of zircon textures. Rev. Mineral. Geochem. 53, 469–500. https://doi.org/10.2113/0530469.
Corfu, F., 2013. A century of U-Pb geochronology: The long quest towards concordance. Geol. Soc. Am. Bull. 125, 33–47. https://doi.org/10.1130/B30698.1.
Cox, S.F., Sun, S.S., Etheridge, M.A., Wall, V.J., Potter, T.F., 1995. Structural and geochemical controls on the development of turbidite-hosted gold quartz vein deposits, Wattle Gully mine, central Victoria, Australia. Econ. Geol. 90, 1722–1746.
Davidson, J.P., Arculus, R., 2006. The significance of Phanerozoic arc magmatism in generating continental crust. M. Brown, T. Rushmer (Eds.), Evolution and Differentiation of the Continental Crust, Cambridge University Press, Cambridge (2006), 135-172.
Ehlers, C., Lindroos, A., Selonen, O., 1993. The late Svecofennian granite-migmatite zone of southern Finland—a belt of transpressive deformation and granite emplacement. Precambr. Res. 64, 295–309. https://doi.org/10.1016/0301-9268(93)90083-E.
Eilu, P., 2012. Gold mineralisation in southwestern Finland. Geol. Surv. Finland Spec. Pap. 52, 11–22.
Eilu, P., Bergman, T., Bjerkgård, T., Feoktistov, V., Hallberg, A., Korsakova, M., Krasotkin, S., Muradymov, G., Nurmi, P.A., Lauri, L.S., Often, M., Perdahl, J.-A., Philippov, N., Sandstad, J.S., Stromov, V., Tontti, M. (comp.), 2016. Metallogenic Map of the Fennoscandian Shield 1:2 000 000. Second edition. Geological Survey of Finland, Geological Survey of Norway, Geological Survey of Sweden, The Federal Agency of Use of Mineral Resources of the Ministry of Natural Resources and Ecology of the Russian Federation.
Gaál, G., Gorbatschev, R., 1987. An outline of the Precambrian evolution of the Baltic Shield. Precambr. Res. 35, 15–52. https://doi.org/10.1016/0301-9268(87)90044-1.
Gale, A., Dalton, C.A., Langmuir, C.H., Su, Y., Schilling, J.G., 2013. The mean composition of ocean ridge basalts. Geochemistry, Geophysics, Geosystems 14 (3), 489–518. https://doi.org/10.1029/2012GC004334.
Goldfarb, R.J., Baker, T., Dube, B., Groves, D.I., Hart, C.J., Gosselin, P., 2005. Distribution, character and genesis of gold deposits in metamorphic terranes. In: Hedenquist, J.W., Thompson, J.F.H., Goldfarb, R.J., Richards, J.P. (Eds.), Economic Geology, 100th Anniversary Volume 407-450.
Goldfarb, R.J., Groves, D.I., 2015. Orogenic gold: Common or evolving fluid and metal sources through time. Lithos 233, 2–26. https://doi.org/10.1016/j.lithos.2015.07.011.
Goldfarb, R.J., Groves, D.I., Gardoll, S., 2001. Orogenic gold and geologic time: a global synthesis. Ore Geol. Rev. 18, 1–75. https://doi.org/10.1016/S0169-1368(01)00016-6.
Gorbatschev, R., Bogdanova, S., 1993. Frontiers in the Baltic Shield. Precambr. Res. 64, 3–21. https://doi.org/10.1016/0301-9268(93)90066-B.
Griffin, W.L., O'Reilly, S., Ryan, C.G., 1999. The composition and origin of sub-continental lithospheric mantle. In Fei, Y., Bertka, C.M., Mysen, B.O. (Eds.), Mantle Petrology: Field Observations and High-pressure Experimentation: a Tribute to Francis R.(Joe) Boyd. Geochemical Society, Special Publication, 6, 13-45.
Griffin, W.L., Pearson, N.J., Belousova, E., Jackson, S.V., Van Achterbergh, E., O'Reilly, S.Y., Shee, S.R., 2000. The Hf isotope composition of cratonic mantle: LAM-MC-ICPMS analysis of zircon megacrysts in kimberlites. Geochim. Cosmochim. Acta 64, 133–147. https://doi.org/10.1016/S0016-7037(99)00343-9.
Griffin, W.L., Wang, X., Jackson, S.E., Pearson, N.J., O'Reilly, S., Xu, X., Zhou, X., 2002. Zircon chemistry and magma mixing, SE China: In-situ analysis of Hf isotopes, Tonglu and Pingtan igneous complexes. Lithos 61 (3–4), 237–269. https://doi.org/10.1016/S0024-4937(02)00082-8.
Groves, D.I., Goldfarb, R.J., Gebre-Mariam, M., Hagemann, S.G., Robert, F., 1998. Orogenic gold deposits: a proposed classification in the context of their crustal distribution and relationship to other gold deposit types. Ore Geol. Rev. 13, 7–27. https://doi.org/10.1016/S0169-1368(97)00012-7.
Guitreau, M., Blichert-Toft, J., Billström, K., 2014. Hafnium isotope evidence for early-Proterozoic volcanic arc reworking in the Skellefte district (northern Sweden) and implications for the Svecofennian orogen. Precambr. Res. 252, 39–52. https://doi.org/10.1016/j.precamres.2014.07.005.
Hermansson, T., Stephens, M.B., Corfu, F., Page, L.M., Andersson, J., 2008. Migratory tectonic switching, western Svecofennian orogen, central Sweden: Constraints from U/Pb zircon and titanite geochronology. Precambr. Res. 161, 250–278. https://doi.org/10.1016/j.precamres.2007.08.008.
Heinonen, A.P., Andersen, T., Rämö, O.T., 2010. Re-evaluation of rapakivi petrogenesis: Source constraints from the Hf isotope composition of zircon in the rapakivi granites and associated mafic rocks of Southern Finland. J. Petrol. 51, 1687–1709. https://doi.org/10.1093/petrology/egq035.
Hollings, P., Ansdell, K., 2002. Paleoproterozoic arc magmatism imposed on an older backarc basin: Implications for the tectonic evolution of the Trans-Hudson orogen, Canada. Geol. Soc. Am. Bull. 114, 153–168. https://doi.org/10.1130/0016-7606(2002)114<0153:PAMIOA>2.0.CO;2.
Hölttä, P., Heilimo, E., 2017. Metamorphic Map of Finland. Bedrock of Finland at the scale 1:1000 000 – Major stratigraphic units, metamorphism and tectonic evolution. Geol. Surv. Finland Spec. Pap. 60, 77–128.
Huhma, H., Claesson, S., Kinny, P.D., Williams, I.S., 1991. The growth of Early Proterozoic crust: new evidence from Svecofennian detrital zircons. Terra Nova 3, 175–178. https://doi.org/10.1111/j.1365-3121.1991.tb00870.x.
Huotari-Halkosaari, T., Nyman, K., Valjus, T., 2016. Uunimäen geofysikaaliset tutkimukset Huittisissa. Geological Survey of Finland, Archive Report 6, 34p (in Finnish).
Kähkönen, Y., Huhma, H., Aro, K., 1989. U-Pb zircon ages and Rb-Sr whole-rock isotope studies of early Proterozoic volcanic and plutonic rocks near Tampere, southern Finland. Precambr. Res. 45, 27–43. https://doi.org/10.1016/0301-9268(89)90029-6.
Kähkönen, Y., 1999. Stratigraphy of the central parts of the Palaeoproterozoic Tampere Schist Belt, southern Finland: review and revision. Bull. Geol. Soc. Finl. 71, 13–29.
Kähkönen, Y., 2005. Svecofennian supracrustal rocks. Developments in Precambrian Geology 14, 343–405. https://doi.org/10.1016/S0166-2635(05)80009-X.
Kara, J., Väisänen, M., Johansson, L., O'Brien, Y.H., Eklund, O., 2018. 1.90-1.88Ga arc magmatism of central Fennoscandia: Geochemistry, U-Pb geochronology, Sm-Nd and Lu-Hf isotope systematics of plutonic-volcanic rocks from southern Finland. Geologica Acta 16, 1–23. https://doi.org/10.1344/GeologicaActa2018.16.1.1.
Kara, J., Väisänen, M., Heinonen, J.S., Lahaye, Y., O'Brien, H., Huhma, H., 2020. Tracing arcloglites in the Paleoproterozoic Era–A shift from 1.88 Ga calc-alkaline to 1.86 Ga high-Nb and adakite-like magmatism in central Fennoscandian Shield. Lithos 372, 105663. https://doi.org/10.1016/j.lithos.2020.105663.
Kärkkäinen, N., Huhta, P., Al-Ani, T., 2015. Uunimäen kultaesiintymän malmimineralogia. Geological Survey of Finland, Archive Report 76, 15p (in Finnish).
Kärkkäinen, N., Koistinen, E., Huotari-Halkosaari, T., Kuusela, J., Muhammad, S., Huhta, P., 2016. Uunimäki gold prospect, Huittinen, Southwest Finland. Geological Survey of Finland, Archive Report 77, 55p.
Kärkkäinen, N., Tiainen, M., 2016. Hydroterminen muuttuminen Hämeen kallioperässä. Geological Survey of Finland, Archive Report 60, 42p (in Finnish).
Kemp, A.I.S., Hawkesworth, C.J., Collins, W.J., Gray, C.M., Blevin, P.L., 2009. Isotopic evidence for rapid continental growth in an extensional accretionary orogen: The Tasmanides, eastern Australia. Earth Planet. Sci. Lett. 284, 455–466. https://doi.org/10.1016/j.epsl.2009.05.011.
Kilpeläinen, T., 1998. Evolution and 3D modelling of structural and metamorphic patterns of the Paleoproterozoic crust in the Tampere-Vammala area, southern Finland. Geological Survey of Finland, Bulletin 397, 1–124.
Koistinen, T.J., 1981. Structural evolution of an early Proterozoic strata-bound Cu-Co-Zn deposit, Outokumpu, Finland. Transactions of the Royal Society of Edinburgh: Earth Sciences 72, 115–158. https://doi.org/10.1017/S0263593300009949.
Koistinen, T., Stephens, M.B., Bogatchev, V., Nordgulen, Ø.,Wennerström, M., Korhonen, J., 2001. Geological map of the Fennoscandian Shield, scale 1:2000 000. Geological Surveys of Finland, Norway and Sweden and the North-West Department of Natural Resources of Russia.

Korja, A., Lahtinen, R., Nironen, M., 2006. The Svecofennian orogen: a collage of microcontinents and island arcs. Geological Society, London, Memoirs 32, 561–578. https://doi.org/10.1144/GSL.MEM.2006.032.01.34.
Korsman, K., Koistinen, T., Kohonen, J., Wennerström, M., Ekdahl, E., Honkamo, M., Idman, H., Pekkala, Y., 1997. Suomen kallioperäkartta–Berggrundskarta över Finland-Bedrock map of Finland. Geological Survey of Finland, Espoo, Finland.
Korsman, K., Korja, T., Pajunen, M., Virransalo, P., GGT/SVEKA Working Group., 1999. The GGT/SVEKA transect: structure and evolution of the continental crust in the Paleoproterozoic Svecofennian orogen in Finland. International Geology Review 41, 287-333. 10.1080/00206819909465144.
Kukkonen, I.T., Lauri, L.S., 2009. Modelling the thermal evolution of a collisional Precambrian orogen: High heat production migmatitic granites of southern Finland. Precambr. Res. 168, 233–246. https://doi.org/10.1016/j.precamres.2008.10.004.
Lahtinen, R., 1994. Crustal evolution of the Svecofennian and Karelian domains during 2.1-1.79 Ga, with special emphasis on the geochemistry and origin of 1.93-1.91 Ga gneissic tonalites and associated supracrustal rocks in the Rautalampi area, central Finland. Geological Survey of Finland, Bulletin 378, 128p.
Lahtinen, R., 1996. Geochemistry of Palaeoproterozoic supracrustal and plutonic rocks in the Tampere-Hameenlinna area, southern Finland. Geological Survey of Finland, Bulletin 389, 113p.
Lahtinen, R., Huhma, H., 1997. Isotopic and geochemical constraints on the evolution of the 1.93-1.79 Ga Svecofennian crust and mantle in Finland. Precambr. Res. 82, 13–34. https://doi.org/10.1016/S0301-9268(96)00062-9.
Lahtinen, R., Korja, A., Nironen, M., 2005. Paleoproterozoic tectonic evolution. Precambrian Geology of Finland 481–532. https://doi.org/10.1016/S0166-2635(05)80012-X.
Lahtinen, R., Korja, A., Nironen, M., Heikkinen, P., 2009a. Palaeoproterozoic accretionary processes in Fennoscandia. Geol. Soc., London, Spec. Publ. 318, 237–256. https://doi.org/10.1144/SP318.8.
Lahtinen, R., Huhma, H., Kähkönen, Y., Mänttäri, I., 2009b. Paleoproterozoic sediment recycling during multiphase orogenic evolution in Fennoscandia, the Tampere and Pirkanmaa belts, Finland. Precambr. Res. 174, 310–336. https://doi.org/10.1016/j.precamres.2009.08.008.
Lahtinen, R., Nironen, M., 2010. Paleoproterozoic lateritic paleosol–ultra-mature/mature quartzite–meta-arkose successions in southern Fennoscandia—intra-orogenic stage during the Svecofennian orogeny. Precambr. Res. 183, 770–790. https://doi.org/10.1016/j.precamres.2010.09.006.
Lahtinen, R., Johnston, S.T., Nironen, M., 2014. The Bothnian coupled oroclines of the Svecofennian Orogen: a Palaeoproterozoic terrane wreck. Terra Nova 26, 330–335. https://doi.org/10.1111/ter.12107.
Lahtinen, R., Huhma, H., Lahaye, Y., Kousa, J., Luukas, J., 2015. Archean-Proterozoic collision boundary in central Fennoscandia: Revisited. Precambr. Res. 261, 127–165. https://doi.org/10.1016/j.precamres.2015.02.012.
Lahtinen, R., Huhma, H., Sipilä, P., Vaarma, M., 2017. Geochemistry, U-Pb geochronology and Sm-Nd data from the Paleoproterozoic Western Finland supersuite–A key component in the coupled Bothnian oroclines. Precambr. Res. 299, 264–281. https://doi.org/10.1016/j.precamres.2017.07.025.
Lamarão, C.N., Dall'Agnol, R., Lafon, J.M., Lima, E.F., 2002. Geology, geochemistry, and Pb–Pb zircon geochronology of the Paleoproterozoic magmatism of Vila Riozinho, Tapajós Gold Province, Amazonian craton, Brazil. Precambr. Res. 119, 189–223. https://doi.org/10.1016/S0301-9268(02)00123-7.
Leskelä, T., 2019. Geochemistry, age determination and structural character of the Au-hosting Uunimäki gabbro, SW Finland. MSc thesis. In: Department of Geography and Geology. University of Turku, p. 84p.
Magni, V., 2019. The effects of back-arc spreading on arc magmatism. Earth Planet. Sci. Lett. 519, 141–151. https://doi.org/10.1016/j.epsl.2019.05.009.
Mäkitie, H., Kärkkäinen, N., Sipilä, P., Tiainen, M., Kujala, H., Klami, J., 2016. Hämeen vyöhykkeen granitoidien luokittelua. Geological Survey of Finland, Archive Report 33, 146p (in Finnish).
Manikyamba, C., Ganguly, S., Santosh, M., Saha, A., Lakshminarayana, G., 2015. Geochemistry and petrogenesis of Rajahmundry trap basalts of Krishna-Godavari Basin, India. Geosci. Front. 6, 437–451. https://doi.org/10.1016/j.gsf.2014.05.003.
McKibbin, S.J., Landenberger, B., Fanning, C.M., 2017. First magmatism in the New England Batholith, Australia: forearc and arc–back-arc components in the Bakers Creek Suite gabbros. Solid Earth 8, 421–434. https://doi.org/10.5194/se-8-421-2017.
Menzies, M.A., Kyle, P.R., Jones, M., Ingram, G., 1991. Enriched and depleted source components for tholeiitic and alkaline lavas from Zuni-Bandera, New Mexico: Inferences about intraplate processes and stratified lithosphere. J. Geophys. Res. Solid Earth 96, 13645–13671. https://doi.org/10.1029/91JB00556.
Mertanen, S., Karell, F., 2011. Rock magnetic investigations constraining relative timing for gold deposits in Finland. Bull. Geol. Soc. Finl. 83, 75–94. https://doi.org/10.17741/bgsf/83.2.001.
Mertanen, S., Karell, F., 2012. Paleomagnetic and AMS studies on Satulinmäki and Koijärvi fault and shearzones. Gold in Southern Finland: Results of GTK Studies 1998–2011. Geol. Surv. Finland Spec. Pap. 52, 195–226.
Middlemost, E.A., 1994. Naming materials in the magma/igneous rock system. Earth Sci. Rev. 37, 215–224. https://doi.org/10.1016/0012-8252(94)90029-9.
Mints, M.V., Glaznev, V.N., Muravina, O.M., Sokolova, E.Y., 2020. 3D model of Svecofennian Accretionary Orogen and Karelia Craton based on geology, reflection seismics, magnetotellurics and density modelling: Geodynamic speculations. Geosci. Front. 11, 999–1023. https://doi.org/10.1016/j.gsf.2019.10.003.
Moghadam, H.S., Li, Q.L., Stern, R.J., Chiaradia, M., Karsli, O., Rahimzadeh, B., 2020. The Paleogene ophiolite conundrum of the Iran-Iraq border region. J. Geol. Soc. 177, 955–964. https://doi.org/10.1144/jgs2020-009.
Mouri, H., Korsman, K., Huhma, H., 1999. Tectono-metamorphic evolution and timing of the melting processes in the Svecofennian Tonalite-Trondhjemite Migmatite belt: An example from Luopioinen, Tampere area, southern Finland. Bull. Geol. Soc. Finl. 71 (1), 31–56.
Nevalainen, J., Väisänen, M., Lahaye, Y., Heilimo, E., Fröjdö, S., 2014. Svecofennian intra-orogenic gabbroic magmatism: a case study from Turku, southwestern Finland. Bulletin of the Geological Society of Finland 86 (2), 93–112.
Nikkilä, K., Korja, A., Koyi, H., Eklund, O., 2015. Analog modeling of one-way gravitational spreading of hot orogens–A case study from the Svecofennian orogen, Fennoscandian Shield. Precambr. Res. 268, 135–152. https://doi.org/10.1016/j.precamres.2015.07.011.
Nironen, M., 1989. The Tampere Schist Belt: structural style within an early Proterozoic volcanic arc system in southern Finland. Precambr. Res. 43, 23–40. https://doi.org/10.1016/0301-9268(89)90003-X.
Nironen, M., Bateman, R., 1989. Petrogenesis and syntectonic emplacement in the early Proterozoic of south-central Finland: a reversely zoned diorite-granodiorite and a granite. Geol. Rundsch. 78, 617–631. https://doi.org/10.1007/BF01776194.
Nironen, M., 1997. The Svecofennian Orogen: a tectonic model. Precambr. Res. 86, 21–44. https://doi.org/10.1016/S0301-9268(97)00039-9.
Nironen, M., 1999. Structural and magmatic evolution in the Loimaa area, southwestern Finland. Bull. Geol. Soc. Finl. 71, 57–71. https://doi.org/10.17741/bgsf/71.1.004.
Nironen, M., 2005. Proterozoic orogenic granitoid rocks. Developments in Precambrian Geology 14, 443–479. https://doi.org/10.1016/S0166-2635(05)80011-8.
Nironen, M., Kousa, J., Luukas, J., Lahtinen, R., 2016. Geological Map of Finland – Bedrock 1:1 000 000. Geological Survey of Finland.
Nironen, M., 2017a. Guide to the geological map of Finland – Bedrock 1:1 000 000. Geol. Surv. Finland Spec. Pap. 60, 41–76.
Nironen, M., 2017b. The Salittu Formation in southwestern Finland, part II: Picritic-basaltic volcanism in mature arc environment. Bull. Geol. Soc. Finl. 89, 5–19. https://doi.org/10.17741/bgsf/89.1.001.
Patchett, P.J., Kouvo, O., Hedge, C.E., Tatsumoto, M., 1982. Evolution of continental crust and mantle heterogeneity: evidence from Hf isotopes. Contrib. Miner. Petrol. 78, 279–297. https://doi.org/10.1007/BF00398923.
Patchett, P.J., White, W.M., Feldmann, H., Kielinczuk, S., Hofmann, A.W., 1984. Hafnium/rare earth element fractionation in the sedimentary system and crustal recycling into the Earth's mantle. Earth Planet. Sci. Lett. 69, 365–378. https://doi.org/10.1016/0012-821X(84)90195-X.
Patchett, J., Kouvo, O., 1986. Origin of continental crust of 1.9-1.7 Ga age: Nd isotopes and U-Pb zircon ages in the Svecokarelian terrain of South Finland. Contrib. Miner. Petrol. 92, 1–12. https://doi.org/10.1007/BF00373959.
Paterson, S.R., Pignotta, G.S., Vernon, R.H., 2004. The significance of microgranitoid enclave shapes and orientations. J. Struct. Geol. 26, 1465–1481. https://doi.org/10.1016/j.jsg.2003.08.013.
Pearce, J.A., Cann, J.R., 1973. Tectonic setting of basic volcanic rocks determined using trace element analyses. Earth Planet. Sci. Lett. 19, 290–300.
Pearce, J.A., 1983. Role of the sub-continental lithosphere in magma genesis at active continental margins. In: Hawkesworth, C., Norry, J. (Eds.), Continental basalts and mantle xenoliths. Shiva Publications, Nantwich, Cheshire, pp. 230–249.
Pearce, J.A., Peate, D.W., 1995. Tectonic implications of the composition of volcanic arc magmas. Annu. Rev. Earth Planet. Sci. 23, 251–286.
Pearce, J.A., 1996. A user's guide to basalt discrimination diagrams. Trace element geochemistry of volcanic rocks: applications for massive sulphide exploration. Geological Association of Canada, Short Course Notes 12, 79–113.
Pearce, J.A., 2008. Geochemical fingerprinting of oceanic basalts with applications to ophiolite classification and the search for Archean oceanic crust. Lithos 100, 14–48. https://doi.org/10.1016/j.lithos.2007.06.016.
Pearson, D.G., Nowell, G.M., 2002. The continental lithospheric mantle: characteristics and significance as a mantle reservoir. Philosophical Transactions of the Royal Society of London. Series A: Mathematical, Physical and Engineering Sciences 360, 2383–2410. https://doi.org/10.1098/rsta.2002.1074.
Peltonen, P., 1995. Petrogenesis of ultramafic rocks in the Vammala Nickel Belt: implications for crustal evolution of the early Proterozoic Svecofennian arc terrane. Lithos 34, 253–274. https://doi.org/10.1016/0024-4937(94)00042-Z.
Peltonen, P., 2005. Svecofennian mafic-ultramafic intrusions. Developments in Precambrian Geology 14, 407–441. https://doi.org/10.1016/S0166-2635(05)80010-6.
Pitkälä, I., 2019. Shear zones and structural analysis of the Loimaa area, SW Finland. MSc thesis. In: Department of Geography and Geology. University of Turku, p. 72p.
Polat, A., Hofmann, A., Rosing, M., 2002. Boninite-like volcanic rocks in the 3.7–3.8 Ga Isua greenstone belt, West Greenland: geochemical evidence for intra-oceanic subduction zone processes in the early Earth. Chem. Geol. 184, 231–254. https://doi.org/10.1016/S0009-2541(01)00363-1.
Pownall, J.M., Hall, R., Lister, G.S., 2016. Rolling open Earth's deepest forearc basin. Geology 44, 947–950. https://doi.org/10.1130/G38051.1.
Rudnick, R.L., Gao, S., 2003. Composition of the continental crust. The crust, Treatise on Geochemistry 3, 1–64.
Rutanen, H., Andersson, U.B., Väisänen, M., Johansson, Å., Fröjdö, S., Lahaye, Y., Eklund, O., 2011. 1.8 Ga magmatism in southern Finland: Strongly enriched mantle and juvenile crustal sources in a post-collisional setting. Int. Geol. Rev. 53, 1622–1683. https://doi.org/10.1080/00206814.2010.496241.
Rutland, R.R., Williams, I.S., Korsman, K., 2004. Pre-1.91 Ga deformation and metamorphism in the Palaeoproterozoic Vammala Migmatite Belt, southern Finland, and implications for Svecofennian tectonics. Bull. Geol. Soc. Finl. 76, 93–140. https://doi.org/10.17741/bgsf/76.1-2.005.

Saalmann, K., 2007. Structural control on gold mineralization in the Satulinmäki and Riukka prospects, Häme Schist Belt, southern Finland. Bull. Geol. Soc. Finl. 79, 69–93. https://doi.org/10.17741/bgsf/79.1.004.

Saalmann, K., Mänttäri, I., Ruffet, G., Whitehouse, M.J., 2009. Age and tectonic framework of structurally controlled Palaeoproterozoic gold mineralisation in the Häme Belt of southern Finland. Precambr. Res. 174, 53–77. https://doi.org/10.1016/j.precamres.2009.06.005.

Saalmann, K., Mänttäri, I., Peltonen, P., Whitehouse, M.J., Grönholm, P., Talikka, M., 2010. Geochronology and structural relationships of mesothermal gold mineralisation in the Palaeoproterozoic Jokisivu prospect, southern Finland. Geol. Mag. 147, 551–569. https://doi.org/10.1017/S0016756809990628.

Salters, V.J., Stracke, A., 2004. Composition of the depleted mantle. Geochem. Geophys. Geosyst. 5 https://doi.org/10.1029/2003GC000597.

Shand, S.J., 1943. Eruptive rocks: their genesis, composition, and classification, with a chapter on meteorites. Wiley, New York, p. 444p.

Sipilä, P., Mattila, J., Tiainen, M., 2011. Pirkanmaan vyöhykkeen ja Hämeen vyöhykkeen välinen terraanirajatulkinta. Geological Survey of Finland, Archive Report 2, 27p (in Finnish).

Sipilä, P., Kujala, H., 2014. Hämeen vyöhykkeen vulkaniittien geokemia. Geological Survey of Finland, Archive Report 119, 23p (in Finnish).

Skyttä, P., Weihed, P., Högdahl, K., Bergman, S., Stephens, M.B., 2020. Paleoproterozoic (2.0–1.8 Ga) syn-orogenic sedimentation, magmatism and mineralization in the Bothnia-Skellefteå lithotectonic unit, Svecokarelian orogen. Geological Society, London, Memoirs 50, 83–130. https://doi.org/10.1144/M50-2017-10.

Smith, E.I., Sanchez, A., Walker, J.D., Wang, K., 1999. Geochemistry of mafic magmas in the Hurricane Volcanic field, Utah: implications for small-and large-scale chemical variability of the lithospheric mantle. J. Geol. 107, 433–448. https://doi.org/10.1086/314355.

Stein, M., Hofmann, A.W., 1994. Mantle plumes and episodic crustal growth. Nature 372, 63–68. https://doi.org/10.1038/372063a0.

Sternai, P., Jolivet, L., Menant, A., Gerya, T., 2014. Driving the upper plate surface deformation by slab rollback and mantle flow. Earth Planet. Sci. Lett. 405, 110–118. https://doi.org/10.1016/j.epsl.2014.08.023.

Stephens, M.B., Andersson, J., 2015. Migmatization related to mafic underplating and intra-or back-arc spreading above a subduction boundary in a 2.0–1.8 Ga accretionary orogen, Sweden. Precambrian Research 264, 235–257. https://doi.org/10.1016/j.precamres.2015.04.019.

Strauss, T.A.L., 2004. The geology of the Proterozoic Haveri Au-Cu deposit, southern Finland. PhD thesis. Rhodes University, p. 306p.

Sun, S.S., McDonough, W.F., 1989. Chemical and isotopic systematics of oceanic basalts: implications for mantle composition and processes. Geological Society, London, Special Publications 42 (1), 313–345. https://doi.org/10.1144/GSL.SP.1989.042.01.19.

Suominen, V., 1988. Radiometric ages on zircons from a cogenetic gabbro and plagioclase porphyrite suite in Hyvinkää, southern Finland. Bull. Geol. Soc. Finl. 60, 135–140.

Tiainen, M., Molnar, F., Koistinen, E., 2013. The Cu-Mo-Au mineralization of the Paleoproterozoic Kedonojankulma intrusion, Häme Belt, Southern Finland. Proceedings of the 12th Biennial SGA Meeting 2, 892-895.

Tiainen, M., Kujala, S., Ahtola, T., Eilu, P., Grönholm, S., Hakala, O., Istolahti, P., Jumppanen, A., Kärkkäinen, N., Rasilainen, K., Törmä, H., 2017. Regional economic impacts of potential mining in Kanta-Häme. Geological Survey of Finland, Research Report 229, 126p.

Torvela, T., Kurhila, M., 2020. How does orogenic crust deform? Evidence of crustal-scale competent behaviour within the partially molten middle crust during orogenic compression. Precambrian Research 342, 105670. https://doi.org/10.1016/j.precamres.2020.105670.

Upton, P., Craw, D., 2014. Extension and gold mineralisation in the hanging walls of active convergent continental shear zones. J. Struct. Geol. 64, 135–148. https://doi.org/10.1016/j.jsg.2013.08.004.

Vaasjoki, M., Huhma, H., 1999. Lead and neodymium isotopic results from metabasalts of the Haveri Formation, southern Finland: evidence for Palaeoproterozoic enriched mantle. Bull. Geol. Soc. Finl. 71, 143–153. https://doi.org/10.17741/bgsf/71.1.007.

Väisänen, M., Mänttäri, I., 2002. 1.90–1.88 Ga arc and back-arc basin in the Orijärvi area, SW Finland. Bull. Geol. Soc. Finl. 74, 185–214. https://doi.org/10.17741/bgsf/74.1-2.009.

Väisänen, M., Skyttä, P., 2007. Late Svecofennian shear zones in southwestern Finland. GFF 129, 55–64. https://doi.org/10.1080/11035890701291055.

Väisänen, M., Westerlund, G., 2007. Palaeoproterozoic mafic and intermediate metavolcanic rocks in the Turku area, SW Finland. Bull. Geol. Soc. Finl. 79, 127–141. https://doi.org/10.17741/bgsf/79.2.001.

Väisänen, M., Kara, J., Penttinen, H., Lahaye, Y., O'Brien, H., Skyttä, P., 2021. U-Pb zircon dating of igneous rocks in the Salo area, SW Finland. In: Extended abstract, 11th Lithosphere Symposium, pp. 151–154.

Vehkamäki, T., Väisänen, M., Kurhila, M., O'Brien, H., Hölttä, P., Syrjänen, J.K., 2021. Metamorphic zones in SW Finland: monazite and zircon U-Pb dating of leucosomes in paragneisses. In: Extended abstract, 11th Lithosphere Symposium, pp. 139–142.

Voipio, T., 2008. Huittisten Palokallion petrografia, malmimineralogia ja geokemia. MSc Thesis, University of Helsinki, 80p. (in Finnish).

Wang, J., Su, Y., Zheng, J., Belousova, E.A., Chen, M., Dai, H., Zhou, L., 2020. Slab roll-back triggered back-arc extension south of the Paleo-Asian Ocean: Insights from Devonian MORB-like diabase dykes from the Chinese Altai. Lithos 376, 105790. https://doi.org/10.1016/j.lithos.2020.105790.

Wasström, A., 1993. The Knaften granitoids of Västerbotten county, northern Sweden. Sveriges geologiska undersökning. Series C: forskningsrapporter 823, 60–64.

Wells, M.L., Hoisch, T.D., Cruz-Uribe, A.M., Vervoort, J.D., 2012. Geodynamics of synconvergent extension and tectonic mode switching: Constraints from the Sevier-Laramide orogen. Tectonics 31 (1). https://doi.org/10.1029/2011TC002913.

Williams, I.S., Rutland, R.R., Kousa, J., 2008. A regional 1.92 Ga tectonothermal episode in Ostrobothnia, Finland: Implications for models of Svecofennian accretion. Precambr. Res. 165, 15–36. https://doi.org/10.1016/j.precamres.2008.05.004.

Wilson, M., 1989. Igneous Petrogenesis. A Global Tectonic Approach, Unwin Hyman, London, p. 464p.

Windley, B.F., Alexeiev, D., Xiao, W., Kröner, A., Badarch, G., 2007. Tectonic models for accretion of the Central Asian Orogenic Belt. J. Geol. Soc. 164, 31–47. https://doi.org/10.1144/0016-76492006-022.

Wood, D.A., Joron, J.L., Treuil, M., 1980. A re-appraisal of the use of trace elements to classify and discriminate between magma series erupted in different tectonic settings. Earth Planet. Sci. Lett. 45, 326–336. https://doi.org/10.1016/0012-821X(79)90133-X.

Xia, L., Li, X., 2019. Basalt geochemistry as a diagnostic indicator of tectonic setting. Gondwana Res. 65, 43–67. https://doi.org/10.1016/j.gr.2018.08.006.

Young, E.D., Anderson, J.L., Clarke, H.S., Thomas, W.M., 1989. Petrology of Biotite-Cordierite-Garnet Gneiss of the McCullough Range, Nevada I. Evidence for Proterozoic Low-Pressure Fluid-Absent Granulite Grade Metamorphism in the Southern Cordillera. J. Petrol. 30, 39–60.